

**ECONOMIC GEOLOGY
RESEARCH UNIT**

University of the Witwatersrand
Johannesburg

— • —

**MAGMA PRODUCTION DURING GRANULITE FACIES
ANATEXIS: DATA FROM "PRIMITIVE"
METASEDIMENTARY PROTOLITHS**

G STEVENS, J D CLEMENS and G T R DROOP

— • INFORMATION CIRCULAR No. 298

UNIVERSITY OF THE WITWATERSRAND
JOHANNESBURG

MAGMA PRODUCTION DURING GRANULITE FACIES ANATEXIS: DATA
FROM "PRIMITIVE" METASEDIMENTARY PROTOLITHS

by

G. STEVENS¹, J.D. CLEMENS² and G.T.R. DROOP³

(*Economic Geology Research Unit, University of the Witwatersrand, Private Bag 3, P O Wits 2050, South Africa.*)

(*School of Geological Sciences, Kingston University, Penrhyn Road, Kingston-upon-Thames, KT12EE, United Kingdom.* ³ *Department of Geology, Manchester University, Manchester, M13 9PL, United Kingdom.)*

ECONOMIC GEOLOGY RESEARCH UNIT
INFORMATION CIRCULAR No. 298

April, 1996

MAGMA PRODUCTION DURING GRANULITE FACIES ANATEXIS: DATA
FROM "PRIMITIVE" METASEDIMENTARY PROTOLITHS

CONTENTS

	Page
INTRODUCTION	1
EXPERIMENTAL TECHNIQUES	3
Starting Materials	3
Experimental Apparatus	5
<i>fO₂</i> Control	7
Observation and Analysis of the Run Products	7
EXPERIMENTAL RESULTS	8
Textures	8
<i>Reactants</i>	8
<i>Products</i>	11
Biotite Fluid-Absent Melting Reactions	11
Biotite Fluid-Absent Melting Interval	12
Phase Chemistry of the Run Products	19
<i>Biotite</i>	19
<i>Garnet</i>	22
<i>Cordierite, Orthopyroxene and Spinel</i>	23
<i>Glass (Quenched Melts)</i>	24
SOURCE-ROCK FERTILITY	32
CONCLUSIONS	35
ABBREVIATIONS	36
ACKNOWLEDGEMENTS	36
REFERENCES	36

____oo____

Published by the Economic Geology Research Unit
Department of Geology
University of the Witwatersrand
1 Jan Smuts Avenue
Johannesburg 2001
South Africa

ISBN 1 86838 202 8

MAGMA PRODUCTION DURING GRANULITE FACIES ANATEXIS: DATA FROM "PRIMITIVE" METASEDIMENTARY PROTOLITHS

ABSTRACT

Fluid absent partial melting experiments have been conducted at 1.0 and 0.5 GPa on a range of relatively magnesian metagreywacke and metapelitic compositions at temperatures appropriate for mid- and lower crustal granulite formation. In metapelites and metagreywackes with Mg#s that vary between 50 and 80 the onset of anatexis occurs under similar conditions. Given relatively reducing, fluid-absent conditions all similar natural metasedimentary granulites should contain evidence of melting if metamorphosed to temperatures of 830 °C. Within the compositional range investigated increasing Mg# raised the temperature of the fluid absent solidus by a maximum of ~ 30 °C. The maximum temperature of biotite-melt coexistence increases with increasing Mg# and the divariant melting interval expands with increasing Mg#. The presence of a Ti component substantially extends the thermal stability range of biotite, but has no discernable effect on the solidus in either bulk composition group. Biotite fluid-absent partial melting in the compositions used in this study produces quartz-saturated granulite-grade assemblages coexisting with water-undersaturated granitic melt. The glass compositions (quenched melt), produced in this study, cluster very tightly. In general the glasses have very similar compositions to those of many natural strongly peraluminous leucogranites.

oOo

MAGMA PRODUCTION DURING GRANULITE FACIES ANATEXIS: DATA FROM "PRIMITIVE" METASEDIMENTARY PROTOLITHS

INTRODUCTION

Migmatisation features that can be interpreted as the products of partial anatexis abound in most quartz-saturated rocks in granulite terranes. Indeed, incongruent melting of hydrous silicates, with internally buffered $\alpha\text{H}_2\text{O}$, to produce a hot, H_2O -undersaturated granitoid magma in conjunction with a less hydrous restitic assemblage, has been proposed as the dominant mechanism of granulite formation (Brown and Fyfe, 1970; Clemens, 1990). The melts produced by this mechanism have the potential to form large-volume, restite-poor plutons, intruded at high crustal levels, or erupting at surface (Brown and Fyfe, 1970; Thompson, 1982) and in some parts of the world e.g. southeastern Australia and southeastern China, such rocks make up 40 to 50% of the exposed crust (Clemens and Vielzeuf, 1987). The migration of large volumes of granitoid magma out of the deep crust has two major consequences. The base of the crust is left in a dehydrated, restitic condition. This zone will be enriched in mafic minerals and characterised by H_2O -poor, granulite-grade mineral assemblages. Such dense rocks would need a second major orogeny, perhaps unrelated to the partial melting event, to become exposed (e.g. the restitic metapelites ("stronalites") of the Ivrea Zone), possibly contributing to the relative scarcity of such rocks, when compared with the abundant mobile magmatic products that they produced. At the same time, the upper crust will become enriched in felsic and heat-producing elements. This is probably the major mechanism for past and ongoing, large-scale crustal differentiation (Vielzeuf *et al.*, 1990). Large-scale melt extraction is not typical of all granulite terranes. Most exposed granulites show little evidence of melt extraction and are more-or-less migmatitic. In such cases some or all of the melt generated during high-grade metamorphism remained *in situ*, often allowing retrograde reactions to partially rehydrate the granulites. Despite this understanding of the role of granulite-grade anatexis in crustal development large areas of uncertainty still surround the process. In particular, there is a lack of knowledge about the possible controls exerted on fluid-absent partial melting equilibria by subtle bulk rock compositional factors, as well as the melting behaviour of relatively magnesian metasedimentary protoliths. This is due to the bias of past experimental investigations towards single, relatively Fe-rich metapelites and metagreywackes, that are similar to the present-day average compositions for these rocks. Despite these similarities in starting materials these past studies have produced some surprisingly disparate results (Table 1).

The past studies of fluid-absent melting in metapelites by Vielzeuf and Holloway (1988) and by Patiño-Douce and Johnston (1991), as well as that by Vielzeuf and Montel (1994) using a metagreywacke starting composition make for interesting comparison. In both sets of experiments on metapelites at 1.0 GPa, significant quantities of melt (> 10%) are present only at temperatures above 800 °C. In the study of Vielzeuf and Holloway (1988), the biotite-out temperature is ~ 850 °C. Above this temperature all the H_2O in the charge is present in the melt phase. Consequently,

melt production is characterised by a large pulse between 825 and 850 °C. In contrast, in the study of Patiño-Douce and Johnston (1991), biotite persisted to a temperature of ~ 975 °C and melt was produced as an approximately linear function of increasing temperature, from 800 °C. Between 1000 and 1100 °C melt proportions in both studies are similar, as might be expected from the similar bulk rock H₂O contents (Table 1). The difference in the upper temperature limit of biotite stability in these two sets of experiments appears to be a function of differences in the bulk rock TiO₂, Na₂O and H₂O contents. The starting materials of Patiño-Douce and Johnston (1991) appear to be ideal for maximising biotite stability. Their runs initially contained 1 vol% ilmenite. The role of TiO₂ in stabilising biotite to higher temperature is well documented (Dymek, 1983; Guidotti, 1984) and this must have contributed to the enhanced biotite stability in these samples. Also, their samples contained an uncharacteristically low plagioclase content (0.43 and 0.4 wt% Na₂O and CaO respectively, as opposed to 1.66 and 1.52 wt% in the rock of Vielzeuf and Holloway (1988). Na is a crucial component in granitic magmas, lowering the solidus over the Na-free system by ~40 °C (Luth, 1976; Johannes and Holtz, 1990). Thus, the Na-poor nature of the bulk composition of Patiño-Douce and Johnston (1991) must favour biotite stability relative to that of granitic melt. This is confirmed by the fact that, even at temperatures as low as 825 °C, they do not record plagioclase in the run products. Their samples were also relatively SiO₂ poor and quartz was often depleted by the melting reaction prior to biotite.

Table 1: Selected results from experiments at 1 GPa in the studies of Vielzeuf and Holloway (VH), (1988), Le Breton and Thompson (LBT), (1988), Patiño-Douce and Johnston (PDJ), (1991) and Vielzeuf and Montel (VM), (1994)

	Starting assem.	Mg#	FA solidus (°C)	wt % H ₂ O	Fe-Partitioning	Kfs product?	Bt out (°C)
VH	Qtz, Pl, Ms, Bt, Chl, St, Grt	41	< 750	1.86	XGrt>XL to 950 °C XL>XGrt to 1100 °C	No	850-862
LBT	Qtz, Pl, Ky, Bt	44	~ 800	1.24	XGrt>XL>XBt(850 °C)	Yes	?
PDJ	Qtz, Pl, Ms, Bt, Als, Grt, Il	36	< 800	1.69	?	No	950-1000
VM	Qtz, Pl, Bt	47	~ 900	1.43	?	No	950-1000

In contrast, biotite stability in the study of Vielzeuf and Holloway (1988) was lowered by the presence of small amounts of staurolite and retrograde chlorite in their starting material. These hydrous minerals break down by subsolidus reactions preceding the anatexis of natural metapelites and their inclusion in the experimental charges implies the presence of a small quantity of free H₂O over and above that necessary to stabilise biotite and muscovite. This is analogous to some small degree of wet melting preceding the fluid-absent breakdown of hydrous phyllosilicates in natural rocks, and must lower the stability of biotite, favouring higher melt fractions.

Previous studies of fluid-absent biotite melting in Al_2SiO_5 -undersaturated rocks have generally used metatonalite compositions (Rutter and Wyllie, 1987; Skjerlie and Johnston, 1992) or involved metagreywackes, but with fluid saturated conditions (Hoschek, 1976; Hoffer and Grant, 1980; Conrad *et al.*, 1988). Only a single fluid-absent investigation has been conducted using a Ca-poor metagreywacke (Vielzeuf and Montel, 1994). This study found that at 1 GPa, fluid-absent melting in the metagreywacke began at ~ 900 °C, suggesting that fluid absent-melting in metagreywackes is unlikely in collisional settings, where temperatures are unlikely to reach 900 °C (e.g. Ashwal *et al.*, 1992), and that fluid-absent melting in metagreywackes probably does not overlap with that in metapelites of the type investigated by Vielzeuf and Holloway (1988).

Collectively these studies indicate the importance of small-scale bulk rock compositional variations on fluid-absent melting behaviour. The variations in the starting materials make it impossible to accurately evaluate differences between anatexis in metapelites and metagreywackes. Likewise, the data do not address the influence of variations in the potentially important variables, bulk rock Mg# and TiO_2 content. This study aims to begin redressing these deficiencies by conducting a series of experiments on biotite fluid-absent melting in a range of relatively magnesian metapelite and metagreywacke compositions. Apart from comparing the melting behaviour in Al_2SiO_5 saturated rocks (metapelites) with that in similar Al_2SiO_5 -free rocks (metagreywackes), the role of variations in bulk rock Mg# ($100 \times \text{Mg}/(\text{Mg}+\text{Fe})$), as well as that of the presence or absence of a TiO_2 component will also be investigated. The main aspects that this investigation concentrates on are: 1) the temperature of initial fluid-absent melting (in field occurrences the temperature of minimum temperature of migmatisation through fluid-absent anatetic processes); 2) the composition of the resultant magmas; and 3) the fertility of the various source materials for the production of granitic magma between the first appearance of melt and a temperature of 1000 °C.

EXPERIMENTAL TECHNIQUES

Starting Materials

Biotite fluid-absent melting was investigated in eight bulk compositions, representing both metapelites and metagreywackes, in the temperature interval between 800 and 1000 °C, and at pressures of 0.5 GPa and 1 GPa. Three synthetic and one natural biotite compositions were used. The synthetic biotites were synthesised from stoichiometric quantities of SiO_2 , Al_2O_3 and carbonates of the alkalis. These were fused to a glass at 1 atmosphere and 1000 °C. The glass was ground, under acetone, with stoichiometric quantities of Fe, Fe_2O_3 and MgO . The resultant dried powders were used to synthesise the biotites hydrothermally at 0.2 GPa and 800 °C in gold capsules. The compositions of the synthetic biotites were determined by microprobe analysis of a glass bead produced by melting a small quantity of biotite powder using an iridium strip heater. Representative compositions of averaged multiple analyses are listed in Table 2. Analysis of the

natural biotite was on single crystals. The H₂O contents of the biotites were determined by thermogravimetry, in argon, on small quantities of the powders dried overnight at a temperature 110 °C, the natural biotite has negligible F and Cl contents.

Table 2: Representative microprobe analyses of the synthetic (A, B and C) and natural biotite (NB) compositions used in this study. The mineral formulae were calculated to 22 oxygen atoms. Analytical procedures are as for the analysis of the run product phase compositions discussed later

wt%	A	B	C	NB
SiO₂	38.28	41.00	42.66	38.18
TiO₂	0.00	0.00	0.00	2.29
Al₂O₃	16.29	14.98	14.75	20.21
FeO	21.34	15.94	8.54	15.34
MgO	11.5	14.81	20.17	12.07
Na₂O	0.36	0.55	0.46	0.00
K₂O	9.28	9.35	9.54	8.99
H₂O	3.51	3.37	3.66	2.92
Total	100.10	100.00	100.00	100.00
Si	5.80	6.04	6.06	5.50
Al⁽⁴⁾	2.23	1.96	1.94	2.50
Al⁽⁶⁾	0.56	0.64	0.52	0.93
Ti	0.00	0.00	0.00	0.25
Fe	2.69	1.96	1.02	1.85
Mg	2.59	3.25	4.27	2.59
Na	0.11	0.16	0.13	0.04
K	1.79	1.76	1.73	1.80
Total	15.77	15.77	15.67	15.46
Mg#	49	62	81	58

Of the eight bulk compositions used, four represent metapelites and contain quartz, plagioclase, sillimanite and biotite. The other four samples are designed to investigate biotite breakdown in metagreywackes and consist of quartz, plagioclase and biotite. The quartz, plagioclase (An = 35) and sillimanite used were picked from a coarse-grained, metapelite-hosted, granulite-grade pegmatite from the Limpopo Belt. The chemical variation within the metapelite and metagreywacke groups results from differences in the biotite compositions used. Three of the samples in each group were created by mixing three synthetic biotite compositions with the other mineral constituents. The powders were prepared by grinding, in an agate ball mill, under acetone,

to an average grain-size of $\leq 5 \mu\text{m}$. A quantity of each starting powder was fused to a homogeneous glass bead, using an iridium strip heater, and analysed by microprobe. The means of multiple analyses are listed in Table 3. The natural whole-rock compositions used in the studies of Patiño-Douce and Johnston (1991), Vielzeuf and Holloway (1988), and Vielzeuf and Montel (1994) are also listed. The bulk-rock H₂O contents were calculated from the measured biotite H₂O contents and the wt% of biotite added to the mixtures. The results were confirmed by thermogravimetric analysis. Aliquots of 100 to 200 mg of sample material were loaded into 10mm long, 3mm OD, 2.8mm ID, gold tubes and dried overnight at 100 °C, prior to immediate crimping and arc welding of the open end. Capsules were weighed before and after experiments to monitor any loss or gain of material and samples showing signs of failure were discarded.

Table 3: Bulk-rock compositions used in the experiments, as well as those used in the studies of Vielzeuf and Holloway (VH), (1988), Patiño-Douce and Johnston (PDJ), (1991), and Vielzeuf and Montel (VM), (1994)

Wt%	Metagreywackes				Metapelites				Previous studies		
	A	B	C	NB	AS	BS	CS	NBS	VH	PDJ	VM
SiO ₂	66.37	67.40	68.03	66.33	58.18	58.93	59.38	58.15	64.35	57.36	69.99
TiO ₂	0.00	0.00	0.00	0.87	0.00	0.00	0.00	0.63	0.82	1.26	0.7
Al ₂ O ₃	12.62	12.35	12.27	14.34	26.42	26.23	26.17	27.67	18.13	23.24	12.96
FeO	8.81	6.76	3.95	6.53	6.57	5.08	3.05	4.92	6.26	8.59	4.87
MnO	0.01	0.01	0.01	0.01	0.01	0.01	0.01	0.01	0.09	0.17	0.06
MgO	4.75	6.01	8.04	4.97	3.45	4.36	5.84	3.61	2.44	2.72	2.36
CaO	1.26	1.19	1.27	1.19	0.91	0.86	0.92	0.86	1.52	0.40	1.67
Na ₂ O	1.31	1.38	1.34	1.17	0.95	1.00	0.98	0.86	1.66	0.48	2.95
K ₂ O	3.58	3.61	3.69	4.48	2.59	2.61	2.66	2.51	2.56	3.63	2.41
H ₂ O	1.33	1.28	1.39	1.11	0.96	0.93	1.01	0.80	2.15	1.69	1.43
Total	100.04	99.99	99.99	100.00	100.04	100.01	100.02	100.02	99.98	99.54	99.40
Mg#	49	62	81	58	49	62	81	58	41	37	47

Experimental Apparatus

The experiments at 0.5 GPa used a Holloway-type, small-volume, internally heated gas vessel, with argon as the pressure medium. The furnace used has a hot-spot of some 4 cm, allowing for simultaneous running of up to six samples. Pressure measurement was by means of a Harwood Engineering manganin cell and home-made bridge, calibrated against a Heise Bourdon-tube gauge and an internal resistance standard. Pressure readings are precise to $< 1 \text{ MPa}$ and believed accurate to $\pm 5 \text{ MPa}$. Temperature was controlled to $\pm 1 \text{ }^\circ\text{C}$ by a Eurotherm 815 controller with automatic cold junction compensation, and measured using two, type K

(chromel-alumel) thermocouples, believed accurate to ± 4 °C. Thermocouples were located adjacent to both ends of the sample capsules. Slight tilting of the pressure vessel (away from the horizontal) during the runs allowed thermal gradients to be maintained at ≤ 3 °C across the capsules, resulting in maximum total temperature uncertainties of ± 7 °C. Runs were brought simultaneously to pressure and temperature and quenched by turning off the furnace power. Runs quenched to 500 °C within 90 seconds, during the quench pressure was maintained by pumping gas into the vessel.

The experiments at 1 GPa used both end-loaded and non-end-loaded piston-cylinder apparatus. Lead-jacketed NaCl-MgO pressure cells were used for all experiments up to 950 °C. Runs at 950 and 1000 °C used lead-jacketed talc-MgO pressure cells. Experiments were performed using both a 1.27 cm pressure vessel, with a single sample arrangement, and a 1.91 cm pressure vessel, allowing for the use of a radial three-sample arrangement. Pressure assemblies in all experiments up to 950 °C comprised an outer, lead-jacketed, NaCl sleeve surrounding the graphite furnace. In the 1.27 cm assembly, the lower half of the furnace was filled with a crushable magnesia rod. The sample packet was placed on top of this and embedded in a small amount of MgO powder. The sample was covered by a 0.5 mm thick ruby disc. The top half of the furnace was filled by a hollow crushable magnesia rod, with the ceramic (recrystallised alumina) sheathed thermocouple support down the centre and the measuring tip butting up against the ruby disc. The tip of the thermocouple was thus placed within 1 mm of the top of the capsule. In other studies, using a similar arrangement, the temperature difference between the sample and the thermocouple was found to be less than 5 °C (Vielzeuf and Montel, 1994). Runs at 950 and 1000 °C used exactly the same assembly, but with talc sleeves replacing the NaCl. In the multi-sample 1.91 cm pressure vessels, a similar NaCl-sleeved graphite furnace was used in runs up to 950 °C. However, the internal diameter of these furnaces was tapered. The top and bottom tapered portions of the furnace were filled by tapered, porous enstatite plugs. The top plug was hollow to allow for the ceramic thermocouple sheaths. Three samples were radially arranged, on a small magnesia spacer, in the gap between the end plugs, with the alumina-sheathed thermocouple protruding down between them. The samples were embedded in MgO powder which also served to isolate them from the thermocouple tip. A second 5 mm OD ceramic sheath covered all but the last 3 mm of the thermocouple to prevent breakage during the run. In all experiments, full pressure was applied prior to heating, with no problems of thermocouple or furnace failure. The hot piston-out technique was employed. Pressure measurement was by a Bourdon-tube gauge and Eurotherm EP90 solid-state digital transducer and process monitor. Pressures were read to ± 1 MPa and are accurate to 4 MPa. A hydraulic pressure controller was used to limit pressure fluctuations to less than ± 1 MPa. Temperature was controlled to ± 1 °C by a Eurotherm 818 controller with automatic cold junction compensation and measured by means of a type R (Pt - PtRh 13%) thermocouple. Total temperature uncertainties are believed to be ± 4 °C.

fO₂ Control

All of the experiments conducted in this study are intended to investigate fluid-absent partial melting. In such systems, redox conditions should be controlled by solid-solid/melt equilibria, and buffer techniques would not normally be employed. Indeed since *fH₂O* is essentially unknown, any form of external *fO₂* control is strictly not possible. However, an early set of 0.5 GPa experiments revealed the common occurrence of magnetite-rich spinel in all supersolidus runs. The abundance of magnetite showed an inverse correlation with Mg#, and distance from the capsule wall in individual samples. No magnetite appeared in the 1 GPa runs using the solid-medium pressure vessel. Thus, the more oxidised state of the lower pressure run products reflects an appreciable H₂ loss through the capsules to the surrounding argon. The most important potential effects of this are: 1) a reduction in the amount of melt present at any given temperature, due to a decrease in the amount of available H₂O (2FeO + H₂O = Fe₂O₃ + H₂); and 2) the preferential stabilisation of the Fe-rich biotite, due to the incorporation of an "oxy" component into these biotites coexisting with melt. Consequently, a technique was devised to counter the loss of H₂ from the capsules. A H₂ diffusion membrane was used in all subsequent 0.5 GPa runs to impose log *fH₂* = -1 relative to the fayalite-magnetite-quartz buffer, at a nominal *aH₂O* = 0.35. As these experiments intend to provide information on fluid-absent biotite melting in reduced, magnesian metasediments, the estimation of the naturally buffered *fO₂* seems reasonable. Also, *aH₂O* = 0.35 seems a reasonable estimate of water activity in anatetic systems buffered by fluid-absent biotite breakdown (e.g. Vielzeuf and Montel, 1994). This technique was designed to minimise the *fH₂* gradient across the capsule walls, thereby eliminating H₂ diffusion out of the capsules. This stratagem eliminated magnetite from the products of all subsequent 0.5 GPa runs. More importantly, it lowered the temperature interval of biotite melt coexistence by up to 30 °C. This effect was most marked in the Fe-rich samples. This technique is a useful refinement of experimental procedure and would probably be of benefit to any future studies involving the fluid-absent melting of Fe-rich biotites or amphiboles, at pressures below 1 GPa. H₂ does not appear to have diffused into the capsules, which were never puffed-up after the runs. If H₂ had diffused into the capsules, this would have possibly reduced an oxide (SiO₂), leading to an increased H₂O supply and the appearance of metallic globules in the charge. No such effects were observed.

Observation and Analysis of the Run Products

Initial examination of the run products, and phase identification, was by XRD analysis and optical grain mount, using a fluid with a refractive index of 1.55 to allow for the easy identification of cordierite. The nature of run products, i.e. either cemented or friable, was used to determine the positions of the solidi in the early experiments. Chips of all the hypersolidus runs were mounted in epoxy resin, sectioned, polished and carbon coated for SEM imaging. The polished sections formed the basis for the detailed analysis of textures and phase compositions produced in the experiments. Phase compositions were obtained using a JEOL JSM 6400 in the

Geology Department at Manchester University, with a Link EXL energy-dispersive analytical system. It is also fitted with an Oxford Instruments cryo-stage. All probe analyses were carried out using an accelerating potential of 15 kV and a probe current of 1.5 nA. To compensate for the weak beam, a large-diameter Be window is fitted to this machine. The counting time was 40 seconds. For the glass analyses, the cryo-stage was used to hold the sample temperature between -192 and -194 °C. These measures appear to eliminate any diffusion-related counting losses of light elements (e.g., Mg, K and Na). Test analyses using this technique produced very similar analyses on both anhydrous and hydrous (9 wt% H₂O) samples of NaAlSi₃O₈ glass (Vielzeuf and Clemens, 1992).

EXPERIMENTAL RESULTS

Textures

The results of the experiments are listed in Table 4a and 4b. No reaction products were observed in the subsolidus runs, the mineral compositions remained unchanged and the grain boundaries resulting from crushing the powders remained visible. In contrast, in the experiments where melting occurred, new phases appeared with the glass (quenched melt), and recrystallisation was extensive. In all cases, all of the phases were in contact with the glass.

Reactants

Quartz occurred as globular rounded crystals that declined in abundance and size with increasing temperature, at 0.5 and 1 GPa. Quartz was depleted in very few experiments.

Plagioclase occurred as rounded crystals of up to 10 mm in runs up to 900 °C. These largest plagioclase crystals are zoned, with more Ca-rich rims. The size and abundance of plagioclase crystals decreased with increasing temperature, in the runs at temperatures above 900 °C, all plagioclase had a skeletal, sponge-like appearance.

Biotite coexisted with the products of the melting reactions in all runs at temperatures close to the solidus. The modal abundance of biotite decreased dramatically with temperature. In the Ti-bearing samples biotite was present as small euhedral crystals up to 5 µm in size. In the Ti-free samples the tiny size of the synthetic biotites seems to have resulted in some degree of biotite aggregation after the final grinding of the powders. This resulted in clusters of biotite flakes up to 20 µm in diameter.

Sillimanite remained present in all metapelitic compositions, but the mineral was consumed during melting and there was no evidence for sillimanite growth.

Table 4a: Run products table for the experiments on metapelites. Unless indicated all the runs contained quartz, sillimanite and plagioclase.
 () = A phase present in minor amounts. (()) = A phase present in trace amounts. Mg#s given in subscripts

Compositions AS		Composition CS							
P(GPa)	T(°C)	Durn.	Assemblage	Comments	P(GPa)	T(°C)	Durn.	Assemblage	Comments
0.5 ± .01	750 ± 2	420	Bt ₄₉		0.5 ± .01	750 ± 2	420	Bt ₈₀	
0.5 ± .01	780 ± 1	392	Bt ₄₈ , (Gl), (Grt), (Crd), (Kfs)		0.5 ± .01	780 ± 1	392	Bt ₇₉ , (Gl), (Crd), (Kfs)	
0.5 ± .01	800 ± 2	290	Bt ₄₉ , Gl ₂₇ , Grt ₃₁ , Crd ₆₁ , Kfs		0.5 ± .01	800 ± 2	290	Bt ₇₈ , Gl ₂₆ , Crd ₃₃ , Kfs	
0.5 ± .01	830 ± 2	296	Gl ₂₉ , Grt ₃₃ , Crd ₆₃ , Kfs		0.5 ± .01	830 ± 2	296	Bt ₇₉ , Gl ₃₀ , Crd ₃₃ , Kfs	
0.5 ± .01	850 ± 2	235	Gl ₂₇ , Grt ₃₆ , Crd ₆₅ , Kfs		0.5 ± .01	850 ± 2	235	Gl ₃₃ , Crd ₈₃ , Kfs	
0.5 ± .01	875 ± 1	170	Gl ₂₂ , Grt ₃₆ , Crd ₆₆ , Kfs		0.5 ± .01	875 ± 1	168	Gl ₃₆ , Crd ₈₃ , (Opx ₈₃), Kfs	Meta Opx
0.5 ± .01	900 ± 2.5	100	Gl ₂₁ , Grt ₃₈ , Crd ₆₉ , Kfs, (Sp ₁₈)		0.5 ± .01	900 ± 2.5	100	Gl ₃₄ , Crd ₈₀ , (Opx ₈₉), (Kfs)	Meta Opx
0.5 ± .01	950 ± 3	78	Gl ₂₁ , Grt ₄₁ , Crd ₇₁ , Sp ₂₀	No Pl	0.5 ± .01	950 ± 3	78	Gl ₄₁ , Crd ₇₇	Meta Opx
0.5 ± .01	1000 ± 4	67	Gl ₁₉ , Crd ₆₅ , Sp ₂₃		0.5 ± .01	1000 ± 4	67	Gl ₃₂ , Crd ₈₂ , ((Opx ₈₈))	Meta Opx
1 ± .007	800 ± 1	163	Bt ₅₂ , (Gl), (Grt ₃₅), (Crd ₆₉)		1 ± .005	800 ± 1	162	Bt ₇₈	
1 ± .007	850 ± 1	146	Bt ₅₇ , (Gl ₃₆), Grt ₃₁ , (Crd ₇₂)		1 ± .007	850 ± 1	146	Bt ₇₉ , (Gl), (Grt ₄₄), (Kfs)	
1 ± .006	900 ± 1	95	Gl ₃₅ , Grt ₄₀ , Crd ₇₃ , Kfs		1 ± .006	900 ± 1	95	Gl ₅₄ , (Grt ₈₃), Crd ₉₀ , Kfs, ((Opx ₈₂))	
1 ± .006	950 ± 1	79	Gl ₄₁ , Grt ₄₂ , ((Opx ₅₇)), Kfs	No Pl	1 ± .009	950 ± 1	78	Gl ₆₃ , Crd ₈₄ , Opx ₅₇	
1 ± .009	1000 ± 1	63	Gl ₅₉ , Grt ₄₆ , Grt ₇₂	No Pl	1 ± .007	1000 ± 1	59	Gl ₆₅ , Crd ₈₇ , Opx ₈₀	
Composition BS									
P(GPa)	T(°C)	Durn.	Assemblage	Comments	P(GPa)	T(°C)	Durn.	Assemblage	Comments
0.5 ± .01	750 ± 2	420	Bt ₅₂		0.5 ± .01	750 ± 2	420	Bt ₅₃	
0.5 ± .01	780 ± 1	392	Bt ₆₄ , Gl, Grt, (Crd), (Kfs)		0.5 ± .01	780 ± 1	392	Bt ₅₈ , ((Gl)), ((Crd))	
0.5 ± .01	800 ± 2	290	Bt ₆₃ , Gl ₃₂ , (Grt), Crd, Kfs		0.5 ± .01	830 ± 2	296	Bt ₄₂ , Gl ₂₁ , ((Grt ₂₇)), Crd ₆₃ , ((Ilm))	
0.5 ± .01	830 ± 2	296	Bt ₅₁ , Gl ₃₉ , Grt ₅₉ , Crd ₈₈ , Kfs		0.5 ± .01	850 ± 2	235	Bt ₄₂ , Gl ₂₂ , ((Grt ₂₇)), Crd ₅₉ , ((Ilm))	
0.5 ± .01	850 ± 2	235	Gl ₂₅ , Grt ₄₀ , Crd ₇₆ , Kfs		0.5 ± .01	875 ± 1	168	Bt ₄₂ , Gl ₂₀ , (Grt ₅₀), Crd ₆₈ , (Ilm)	
0.5 ± .01	875 ± 1	168	Gl ₂₂ , Grt ₄₂ , Crd ₇₁ , Kfs		0.5 ± .01	900 ± 2.5	100	Gl ₄₃ , Crd ₇₆ , (Ilm)	
0.5 ± .01	900 ± 2.5	100	Gl ₃₃ , Grt ₅₇ , Crd ₇₃ , (Kfs), (Sp ₁₇)		0.5 ± .01	950 ± 3	78	Gl ₄₃ , Crd ₇₂ , (Ilm)	
0.5 ± .01	950 ± 3	78	Gl ₃₁ , Crd ₇₀ , Sp ₂₁		0.5 ± .01	1000 ± 4	67	Gl ₄₆ , Crd ₇₂ , (Ilm)	
0.5 ± .01	1000 ± 4	67	Gl ₂₆ , Crd ₇₀ , (Sp ₂₆)		1 ± .021	800 ± 1	214	Bt	
1 ± .005	800 ± 1	165	Bt		1 ± .008	850 ± 1	150	Bt ₆₃ , ((Gl)), Grt ₄₀ , (Crd ₃₅), ((Ilm))	
1 ± .008	850 ± 1	150	Bt ₇₂ , (Gl ₄₃), Grt ₄₀ , Crd ₇₇ , (Kfs)		1 ± .007	900 ± 1	125	Bt ₆₈ , Gl ₅₁ , Grt ₄₃ , (Ilm)	
1 ± .007	900 ± 1	96	Gl ₅₆ , Grt ₅₂ , Crd ₇₈ , ((Opx ₇₂)), Kfs	Meta Opx	1 ± .006	950 ± 1	79	Gl ₆₇ , Grt ₅₃ , Opx ₇₀ , (Ru)	
1 ± .006	950 ± 1	79	Gl ₄₉ , Grt ₅₆ , Crd ₈₀		1 ± .004	1000 ± 1	115	Gl ₇₅ , Opx ₈₅ , (Ru)	No Pl, Qz
1 ± .007	1000 ± 1	63	Gl ₅₆ , Grt ₆₂ , (Opx ₇₇)	No Pl					

Table 4b: Run products table for the experiments on metagreywackes

Composition A						Composition C					
P(GPa)	T(°C)	Durn.	Assemblage	Comments	P(GPa)	T(°C)	Durn.	Assemblage	Comments		
0.5 ± .01	800 ± 3	323	Bt		0.5 ± .01	800 ± 3	323	Bt			
0.5 ± .01	835 ± 2	304	Bt _{ss} , Gl ₄₂ , Grt ₄₄ , Opx ₅₃ , (Crd ₆₂), Kfs		0.5 ± .01	835 ± 2	304	Bt ₇₉ , (Gl), (Crd ₈₀), Opx ₇₃ , (Kfs)			
0.5 ± .01	850 ± 2	247	Gl ₄₄ , Grt ₃₉ , Opx ₄₈ , Crd ₇₃ , Kfs		0.5 ± .01	850 ± 2	247	Bt ₇₉ , Gl ₇₉ , (Crd ₈₀), Opx ₇₃ , (Kfs)			
0.5 ± .01	875 ± 5	225	Gl ₂₇ , Grt ₃₇ , Opx ₅₁ , Kfs		0.5 ± .01	875 ± 5	225	Gl _{ss} , Crd ₈₇ , Opx ₇₇ , Kfs			
0.5 ± .01	900 ± 1	174	Gl ₃₅ , Grt ₃₄ , Opx ₅₀		0.5 ± .01	900 ± 1	174	Gl _{ss} , Crd ₈₇ , Opx ₇₆ , Kfs			
0.5 ± .01	950 ± 3	149	Gl ₃₁ , (Grt ₅₅), Opx ₄₈		0.5 ± .01	950 ± 3	149	Gl ₆₅ , Crd ₈₈ , Opx ₇₇			
0.5 ± .01	1000 ± 2	122	Gl ₂₈ , Opx ₅₅	No Pl	0.5 ± .01	1000 ± 2	122	Gl ₅₀ , Crd ₈₈ , Opx ₈₁			
1 ± .005	780 ± 1	296	Bt		1 ± .007	780 ± 1	310	Bt			
1 ± .004	800 ± 1	256	Bt ₅₂ , (Gl), (Grt)		1 ± .012	800 ± 1	208	Bt ₈₀ , ((Gl)), ((Grt))			
1 ± .012	850 ± 1	168	Gl ₃₃ , Grt ₃₅ , Opx ₅₆ , Kfs		1 ± .015	850 ± 1	128	Bt ₅₂ , (Gl), (Grt ₅₂), Ksp			
1 ± .007	875 ± 1	120	Gl ₃₈ , Grt ₃₇ , Opx ₅₁ , Kfs		1 ± .007	875 ± 1	102	(Bt), Gl ₄₇ , Crd ₆₇ , Opx ₅₉ , Ksp			
1 ± .007	900 ± 1	127	Gl ₃₉ , Grt ₄₁ , Opx ₅₃ , Kfs		1 ± .009	900 ± 1	143	Gl ₅₂ , Grt ₆₆ , Opx ₈₁ , Ksp			
1 ± .009	950 ± 1	83	Gl ₅₂ , Grt ₅₈ , Opx ₅₇		1 ± .009	950 ± 1	83	Gl _{ss} , Opx ₅₈			
1 ± .004	1000 ± 1	71	Gl ₅₄ , Grt ₄₅ , Opx ₅₂	No Pl	1 ± .004	1000 ± 1	93	Gl _{ss} , Opx ₈₁			

Composition B						Composition NB					
P(GPa)	T(°C)	Durn.	Assemblage	Comments	P(GPa)	T(°C)	Durn.	Assemblage	Comments		
0.5 ± .01	800 ± 3	323	Bt		0.5 ± .01	800 ± 3	323	Bt			
0.5 ± .01	835 ± 2	304	Bt ₆₇ , ((Gl)), ((Opx))		0.5 ± .01	835 ± 2	304	Bt ₆₄ , (Gl), (Grt ₃₂), Crd ₇₃ , (Opx), (Ilm)			
0.5 ± .01	850 ± 2	247	Gl ₄₁ , (Grt ₄₂), Opx ₆₁ , Crd ₈₈ , Kfs		0.5 ± .01	850 ± 2	247	Bt ₆₁ , Gl ₅₉ , Crd ₆₇ , Opx ₅₄ , (Ilm)			
0.5 ± .01	875 ± 5	225	Gl ₅₆ , Opx ₅₂ , Kfs		0.5 ± .01	875 ± 5	225	Bt ₅₉ , Gl ₃₂ , Crd ₇₃ , Opx ₅₃ , (Ilm)			
0.5 ± .01	900 ± 1	174	Gl ₃₄ , Opx ₅₁		0.5 ± .01	900 ± 1	174	Bt ₅₈ , Gl ₃₄ , (Grt ₃₀) Opx ₅₁ , (Ilm)			
0.5 ± .01	950 ± 3	149	Pl, Gl ₄₃ , Opx ₆₂		0.5 ± .01	950 ± 3	149	Gl ₃₂ , Opx ₆₀ , (Ilm) No Qtz, Pl			
0.5 ± .01	1000 ± 2	122	Gl ₄₀ , Opx ₅₇ , (Crd ₈₈)		0.5 ± .01	1000 ± 2	122	Gl ₄₄ , Opx ₅₅ , (Ilm) No Qtz, pl			
1 ± .009	800 ± 1	253	Bt ₆₆		1 ± .007	800 ± 1	236	Bt			
1 ± .014	850 ± 1	162	Bt ₆₈ , (Gl), Grt ₄₂ , Opx ₆₃ , ((Kfs))		1 ± .008	850 ± 1	150	Bt ₆₇ , (Gl ₃), Grt ₃₈ , Crd ₇₄ , ((Ilm))			
1 ± .007	875 ± 1	115	Gl ₃₆ , Grt ₄₇ , Opx ₇₁ , Kfs		1 ± .007	875 ± 1	163	Bt ₇₁ , Gl ₃₈ , Grt ₄₅ , ((Ilm))			
1 ± .006	900 ± 1	122	Gl ₃₂ , Grt ₄₈ , Opx ₆₉ , Kfs		1 ± .007	900 ± 2	144	Bt ₇₁ , Gl ₄₇ , Grt ₄₇ , (Ilm)			
1 ± .009	950 ± 1	83	Gl ₃₃ , Grt ₄₉ , Opx ₆₆		1 ± .018	950 ± 1	118	Gl ₅₇ , Grt ₅₄ , Opx ₇₁ , (Ru) No Pl			
1 ± .004	1000 ± 1	70	Gl ₃₉ , Grt ₅₄ , ((Grt ₂₅)), Opx ₇₃ , No Pl		1 ± .009	1000 ± 1	101	Gl ₄₂ , Opx ₅₁ , (Ru) No Pl			

Products

Glass was present in all the hypersolidus runs and increased in abundance with increasing temperature. The glass has a deep brown colour in grain mount and invariably contains some rounded bubbles. These are interpreted to represent some atmosphere sealed into the capsule. The bubbles were present in runs at 0.5 and 1 GPa.

Cordierite was produced as a major product of the melting reactions in all samples at 0.5 GPa, and in the metapelites and Mg-rich metagreywackes at 1 GPa. The abundance of cordierite decreased with increasing temperature and pressure. Cordierite occurred as euhedral, rectangular or hexagonal shaped crystals, between 3 and 20 μm in size.

Garnet occurred as euhedral poikilitic crystals, up to 15 μm in diameter, with abundant small inclusions of quartz and glass. The new garnet growth generally nucleated on the seed crystals. The seeds remained chemically distinct and were usually more Fe-rich than the new rims. Garnet abundance correlated positively with increasing pressure.

Orthopyroxene was generally present in the "metagreywacke" hypersolidus runs as euhedral, elongated prisms between 3 and 20 μm in length. Orthopyroxene abundance increased with increasing pressure.

K-feldspar was present in the temperature interval between the solidi and 900 - 950 °C in all the experiments using Ti-free compositions. Close to the solidus temperatures it occurred as small euhedral crystals, occasionally as large as 6 μm in length, but became sponge-like close to 900 °C. In the Ti-bearing compositions, K-feldspar was not present at the solidus but appeared between 875 and 900 °C as melting progressed. In these compositions it also disappeared below 950 °C. K-feldspar was often observed to have nucleated on plagioclase seeds.

At temperatures above the solidi, all the experiments using natural Ti-bearing biotite contain a Ti-rich phase, other than biotite. In most runs ilmenite occurred as small globular crystals up to 3 μm in diameter. In 1 GPa experiments at 950 °C rutile was present in place of ilmenite.

Spinel was produced as a minor phase in compositions AS and BS from runs at 0.5 GPa and 900 °C.

Biotite Fluid-Absent Melting Reactions

The phase changes produced in the fluid-absent melting interval with increasing temperature suggest that two general melting reactions can be proposed for biotite breakdown in this study. In the "metapelite" samples, and with Ti-free compositions, the reaction appears to be:



In the Ti-free "metagreywacke" samples the reaction is:



The reactions are very similar in the respective Ti-bearing compositions. In the case of these samples, however, small amounts of ilmenite are produced and K-feldspar is only present in the runs from 900 °C. These reactions are very similar to those proposed for metasediments on the grounds of theoretical modelling (Fyfe, 1973; Grant, 1985; Clemens and Vielzeuf, 1987) and

those proposed in previous experimental investigations on more Fe-rich metapelite and metagreywacke compositions (Vielzeuf and Holloway, 1988; Le Breton and Thompson, 1988; Patiño-Douce and Johnston, 1991; Vielzeuf and Montel, 1994). If the magnesian nature of the present compositions is taken into account, the reactions also agree well with those suggested for biotite breakdown on the basis of petrographic investigations of migmatised metasedimentary granulites (Stevens and Van Reenen, 1992; Srogi *et al.*, 1993).

Biotite Fluid-Absent Melting Interval

The influence of the bulk compositional variables on the fluid-absent metapelite and metagreywacke solidi, as well as on the upper temperature of biotite-melt coexistence are illustrated in Figure 1. In runs with very low melt proportions (< 5%) the melt is difficult to identify. The presence of new growth of a ferromagnesian phase less hydrous than biotite, as well as the non-friable nature of such samples, was taken as evidence that some melting had occurred. In both the metapelite and metagreywacke sample groups, bulk rock Mg# appears to raise the solidus temperature slightly (Figs. 2, 3). Across the range of compositions investigated this increase is approximately 30 °C. The data also clearly indicate that the presence or absence of a Ti-component in biotite does not appear to influence the beginning of melting. The Mg# of composition NB/NBS (58) is most closely matched by that of composition B/BS (62). In both the metapelites and the metagreywackes, the solidi behaviour of the Ti-bearing and Ti-free samples are indistinguishable within the resolution of the experiments (Fig. 3). These Mg# and TiO₂ effects appear to be consistent in the metapelites and metagreywackes at both 0.5 and 1.0 GPa. At 0.5 GPa there is a significant difference between the temperature of the metagreywacke and metapelite solidi. Biotite fluid-absent melting in the metapelites occurs some 50 °C below that in the metagreywackes at this pressure (Fig. 1). At 1 GPa there is no discernible difference between the solidus temperatures of the two systems. The degree to which the presence of sillimanite depresses the solidus appears to be a function of pressure. This is possibly due to the fact that the melting reaction in the metapelites consumes more sillimanite at the lower pressure, because it produces more cordierite (less garnet) under these conditions. The result of this difference between the observed effects at 0.5 and 1 GPa is that the data appear to support a steep positive dP/dT slope for biotite fluid-absent melting in metapelites, raising the possibility of decompression melting in this system, while suggesting a steep negative dP/dT slope for biotite fluid-absent melting in metagreywackes.

The effect of the presence of sillimanite on the upper limit of biotite stability seems to mimic the effect of this variable on the metapelite solidus, as the biotite-out curves for all compositions appear to have steep positive dP/dT slopes (Fig. 1). The data support a strong Mg# control on the upper stability limit of biotite. In both bulk-rock composition groups, increasing Mg# raises the maximum temperature of biotite-melt coexistence. In the metagreywackes this trend appears to be more marked at 1 GPa than at 0.5 GPa. TiO₂ in biotite has a dramatic effect in raising the

upper limit for the coexistence of biotite and H_2O -undersaturated melt. In the Ti-free metagreywacke compositions at 850 °C and 0.5 GPa only C contains a small percentage of biotite; in the two more Fe-rich compositions biotite has disappeared from the assemblage. However, in the Ti-bearing composition, NB, a significant proportion of biotite still remains (Fig. 4). The magnitude of the stabilising influence of TiO_2 in biotite can be gauged by comparing the upper stability limit of the natural biotite NB ($\text{Mg}\# = 58$) to that of the synthetic biotite B ($\text{Mg}\# = 62$). The data suggest an increase of the order of 75 °C, in the case of biotite in metapelites, and about 100 °C for biotite in metagreywackes.

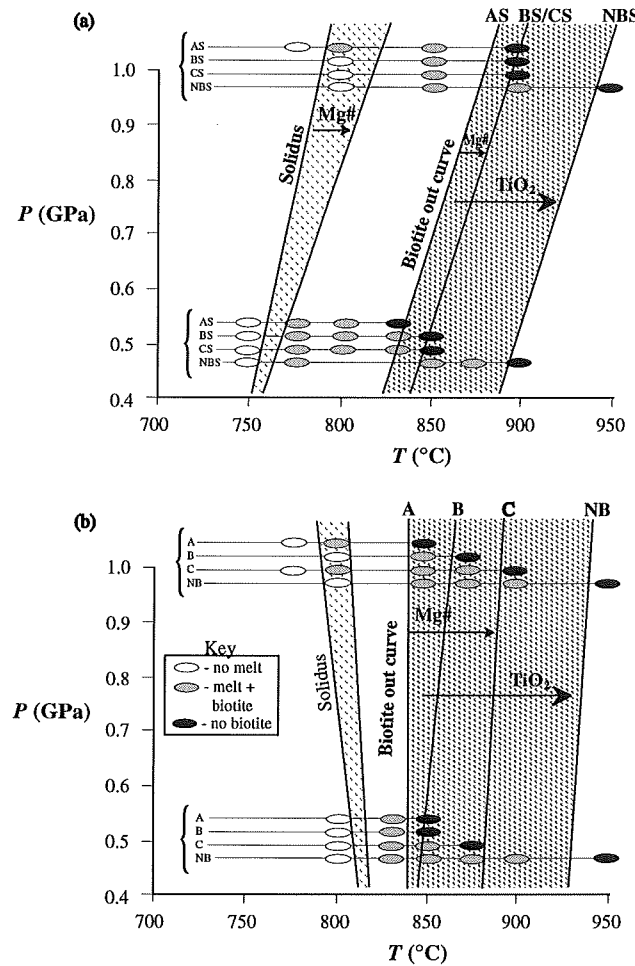


Figure 1: Results of experiments investigating the position of the metapelite (a) and metagreywacke (b) solidi, as well as the upper-limit of biotite stability in all compositions. $\text{Mg}\#$ exerts a strong control on the maximum thermal stability of biotite. Ti in biotite does not influence the position of the solidus, but enhances the upper limit of biotite-melt coexistence markedly. The collective effects of $\text{Mg}\#$ and TiO_2 on the upper limits of biotite stability are indicated by the high-temperature shaded field.

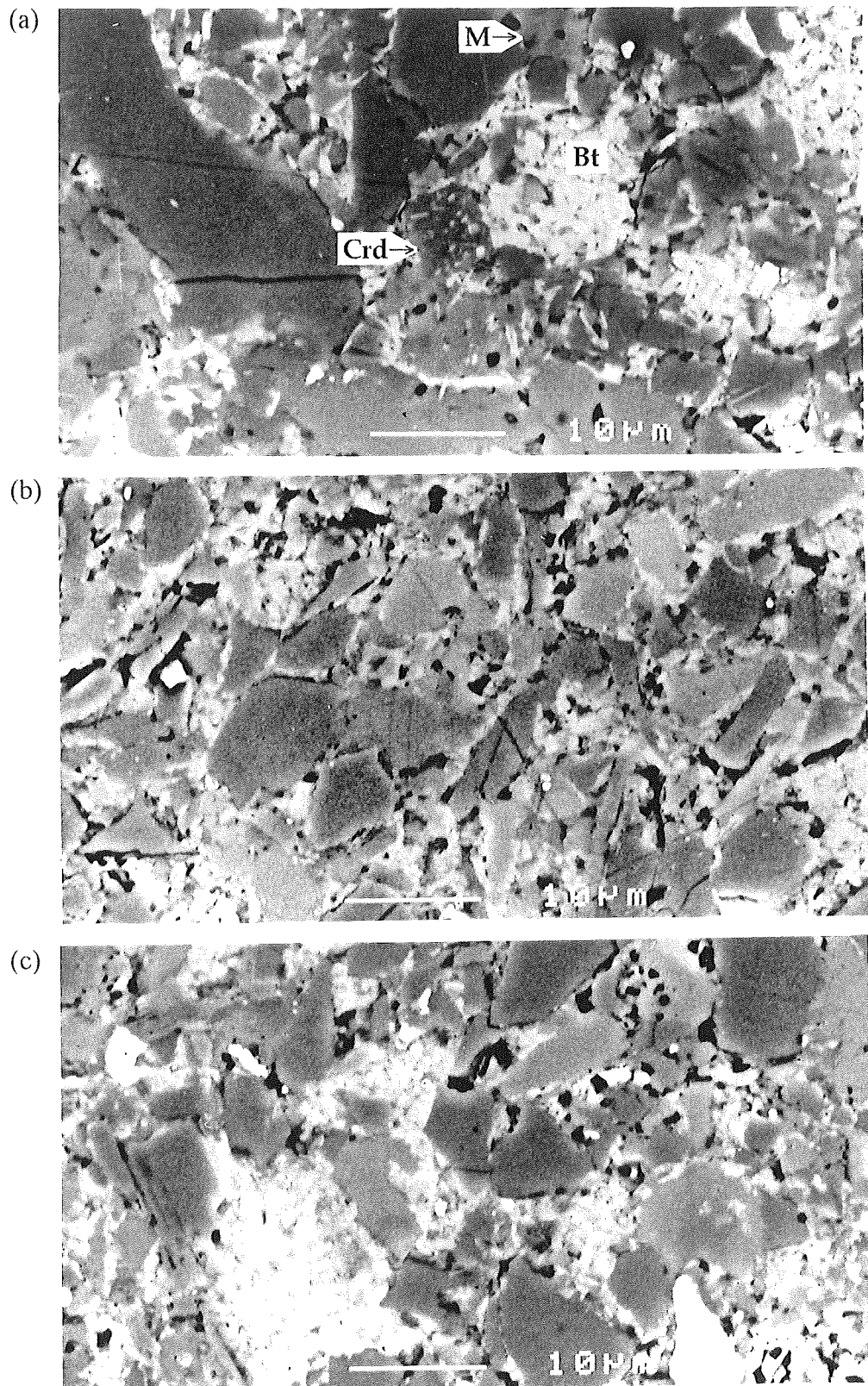
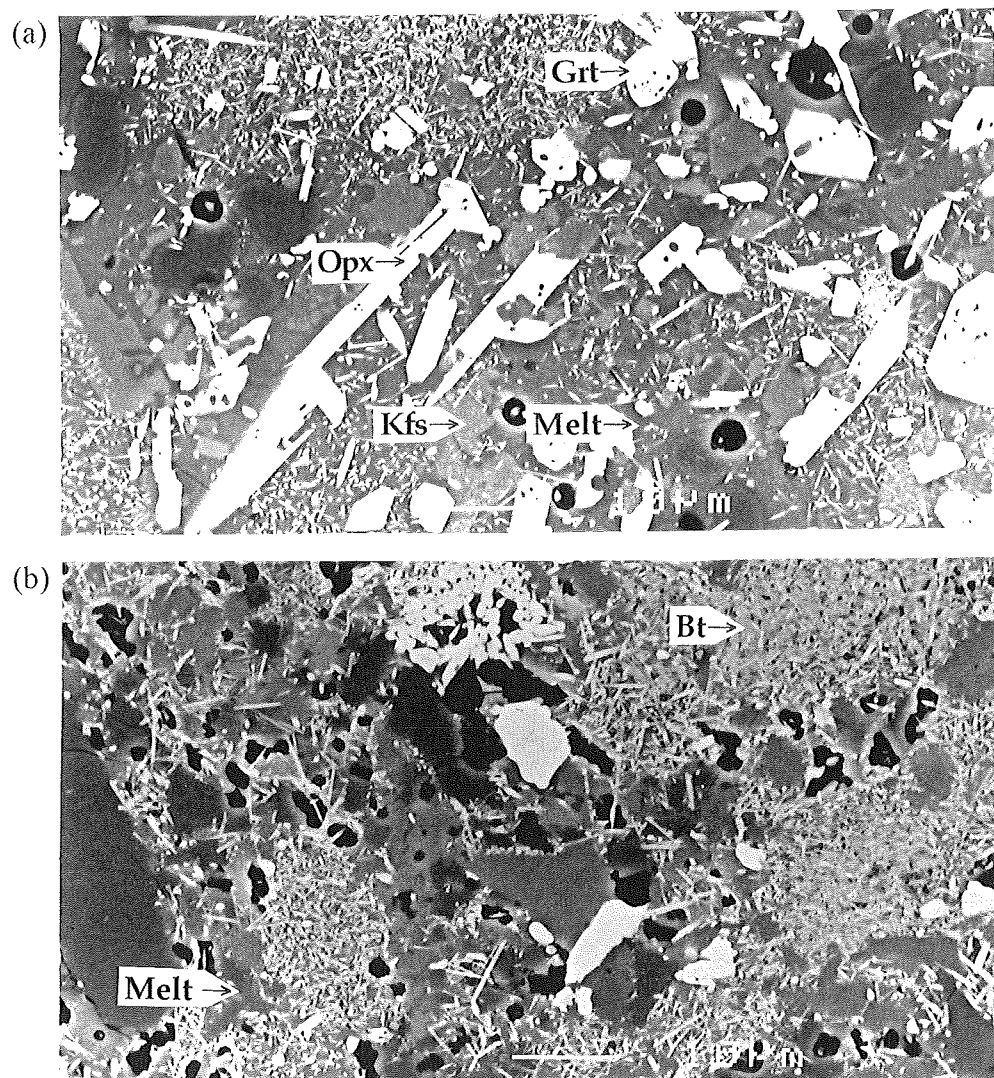


Figure 2: Back-scattered SEM images of run products from AS (a), BS (b) and CS (c) at 0.5 GPa and 780 °C. All have produced some melt at the biotite fluid-absent solidus. AS, however, appears to have melted more than BS or CS. Note the aggregated biotite (Bt), the melt menisci (M), and the cordierite crystal (Crd) that coexisted with biotite and melt in AS.



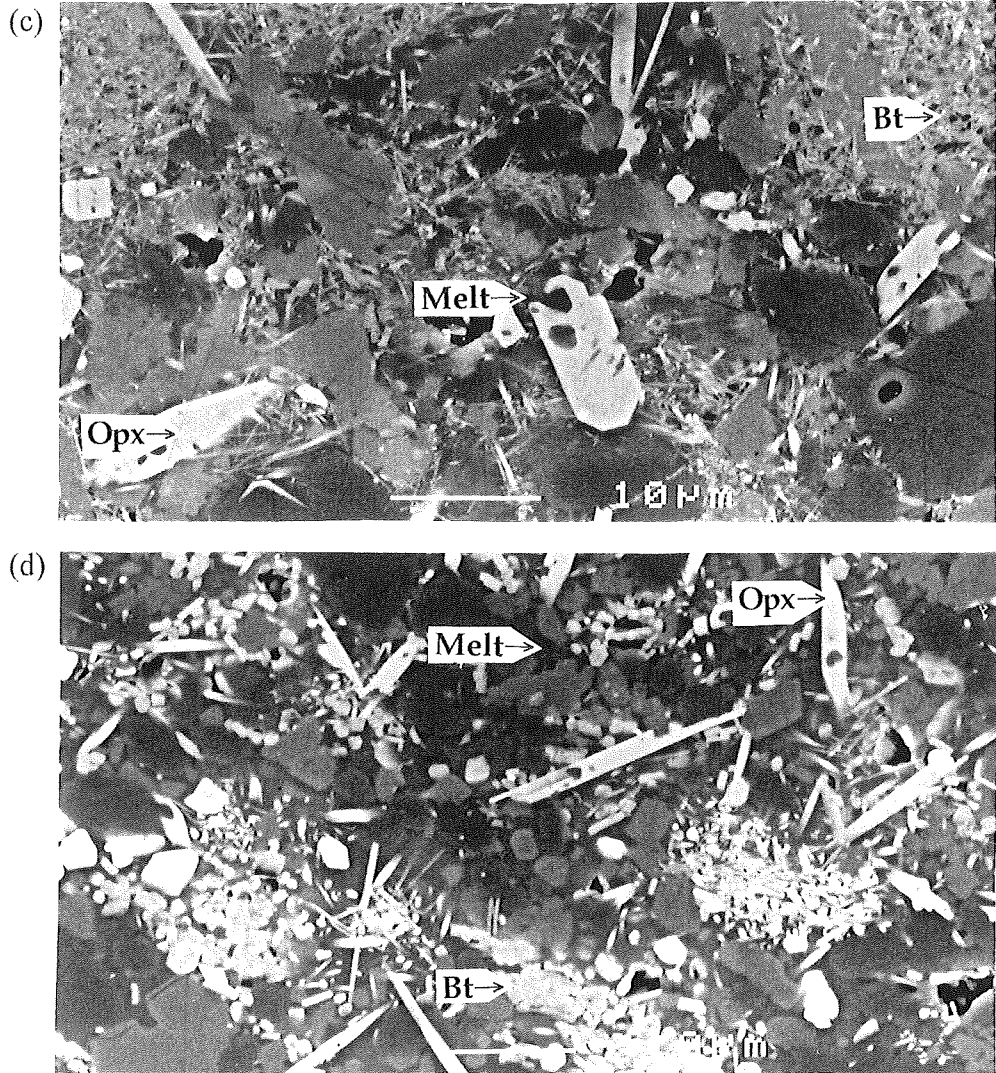
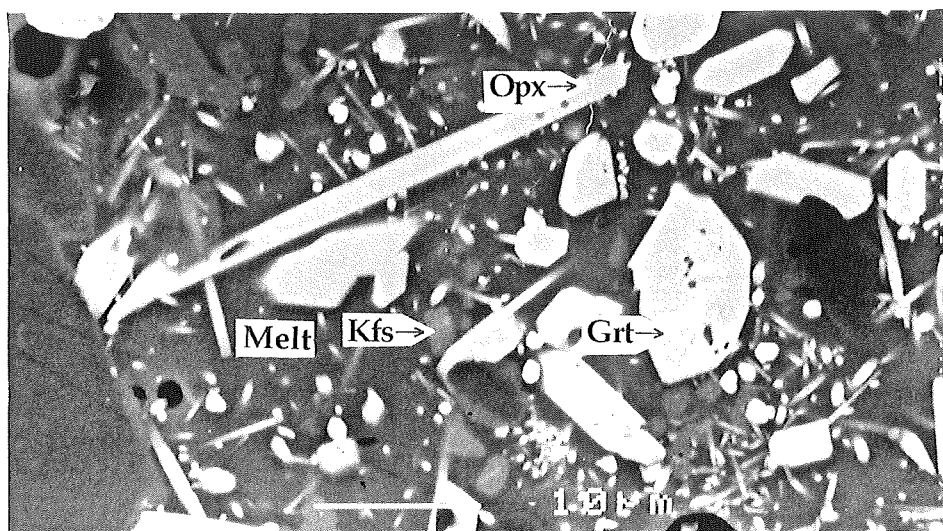
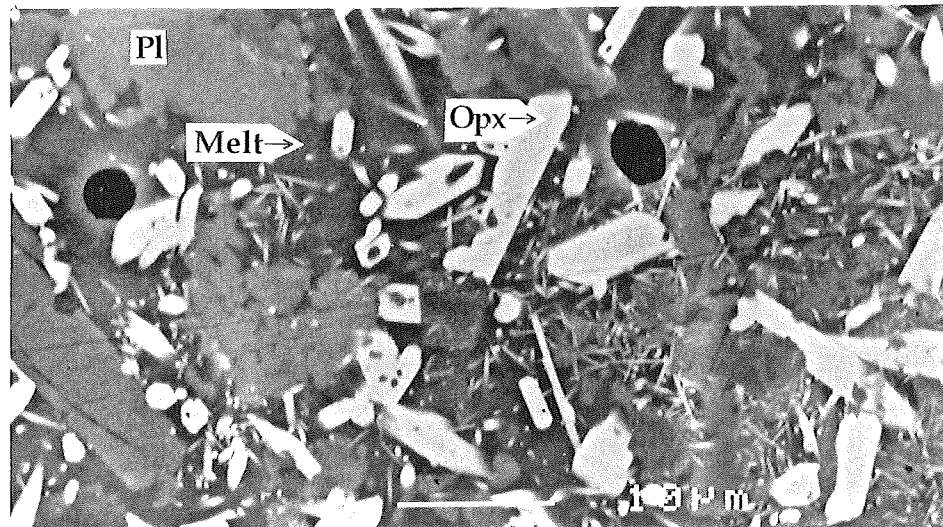


Figure 3: Back-scattered SEM images of the run products from metagreywackes A (a), B (b), C (c) and NB (d) at 0.5 GPa and 835 °C. Melting in A is well progressed and only a trace of biotite remains. From the resultant mineralogy, the melting reaction appears to be $Bt + Qtz + Pl = Melt + Opx + Grt + Crd + Kfs$. In composition B biotite has melted very little at the same conditions. This is reflected in the higher proportion of biotite remaining and the less well recrystallised nature of the run products. In common with composition B, melting in C is not extensive and a high proportion of biotite remains. In this more Mg-rich composition the melting reaction appears to be $Bt + Qtz + Pl = Melt + Opx + Crd + Kfs$. In the Ti-bearing composition, (NB), biotite fluid-absent melting has progressed further than in the Ti-free, more Mg-rich compositions B and C. This illustrates the lack of a TiO_2 control on the position of the solidus. If the presence of a TiO_2 component in biotite does raise the fluid-absent solidus at all, the effect appears secondary to that of bulk-rock Mg#.

(a)



(b)



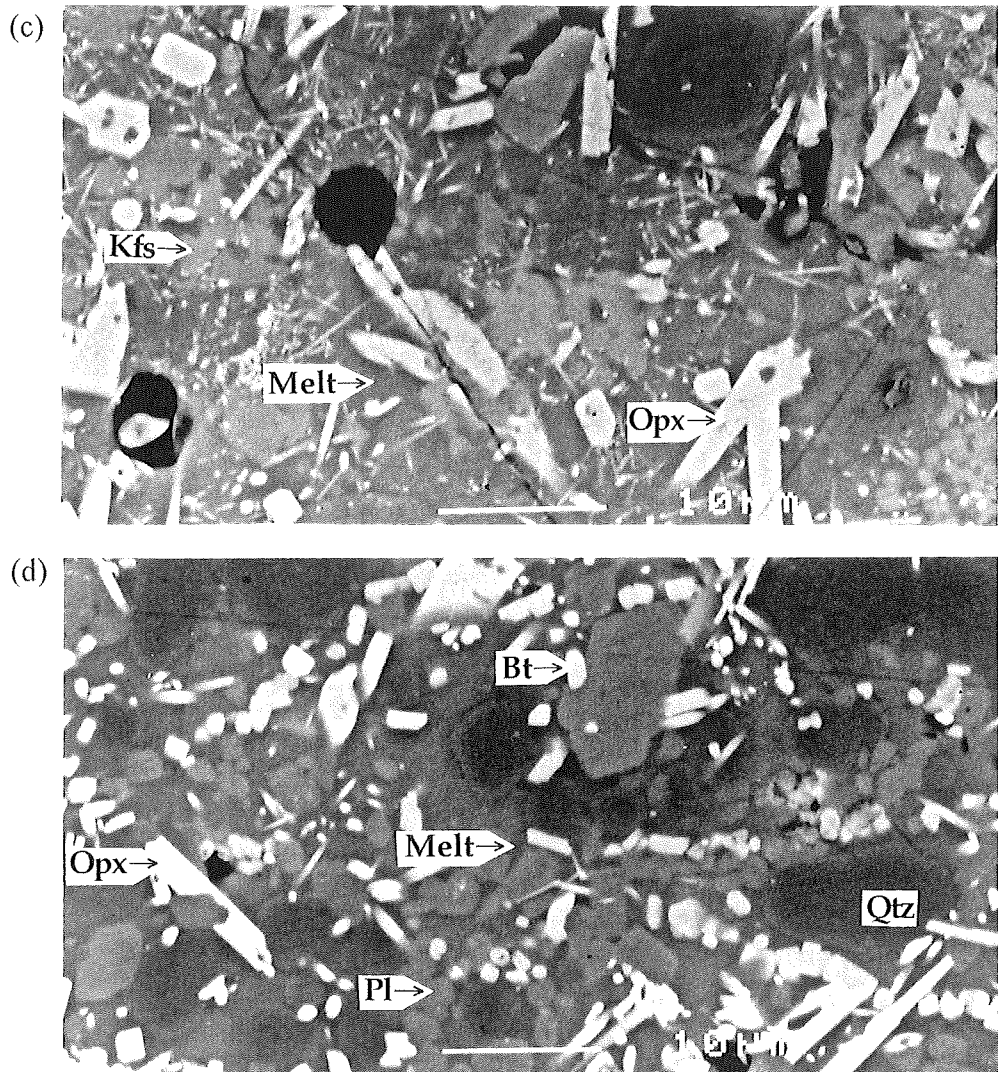


Figure 4: Back-scattered SEM images from experiments on metagreywackes A (a), B (b), C (c) and NB (d) at 0.5 GPa and 850 °C. In the three Ti-free samples biotite fluid-absent melting has progressed to completion (a trace of biotite remains in C). However, in the Ti-bearing sample, NB, (intermediate to A and B in terms of Mg#) a substantial amount of biotite remains. A comparison of the melt fractions in B and C with those in the same compositions illustrated in Figure 3 (830 °C at 0.5 GPa), stresses the abrupt nature of biotite breakdown in the Ti-free samples

Phase Chemistry of the Run Products

A database listing the glass compositions and the compositions of all the solid solution minerals produced in most of the hypersolidus experiments is available on request from the authors. Only important trends in phase compositions and the compositions of the glasses are given in this paper.

Biotite

Variations across the melting interval in biotite Mg#, Al partitioning and, in the case of the titaniferous biotite, TiO₂ concentration, are similar to those described by Patiño-Douce *et al.* (1993). In samples where biotite and garnet coexisted, biotite becomes preferentially enriched in Mg across the melting interval. TiO₂ content increases with increasing temperature. Al in octahedral co-ordination decreases with increasing temperature, and increases as a function of pressure. Patiño-Douce *et al.* (1993) proposed the operation of the substitution $0.66\text{Al}(6) + 0.33\square = (\text{Fe}, \text{Mg})$ to explain the incorporation of octahedral Al into their biotites. Data from the Ti-free, synthetic biotite runs in this study appear to correlate perfectly with the trend that would be expected for this substitution (Fig. 5a); however, the analyses for the natural, Ti-bearing biotite samples scatter widely and do not accurately define a trend. These biotites all contain significant amounts of Ti, probably in octahedral co-ordination. In contrast to Al(6), Ti contents of the biotites increase with increasing temperature, and there is thus an inverse correlation between Ti and Al(6) content in the biotites produced in this study (Fig. 6). These data define a linear trend with a slope that is consistent with $\text{Al}(6) = 0.75\text{Ti}$, possibly indicating a direct, vacancy-inducing, charge-balanced exchange between Al and Ti in the octahedral sites. If Ti + Al(6) are plotted against Fe + Mg, the data for the natural Ti-bearing biotites also define a linear trend (Fig 5b). The slope of this linear trend is consistent with the resultant proposed substitution for the natural titaniferous biotite of $0.5\text{Ti} + 0.66\text{Al} + 0.83\square = 2(\text{Fe}, \text{Mg})$. This appears to be the mechanism by which the thermal stability of titaniferous biotite is enhanced. In the experiments where garnet and biotite coexisted Fe-Mg partitioning was compared to that predicted by the geothermometer of Ferry and Speer (1978). The data from this study plot close to the extrapolated trend of the data on which the geothermometer is based and well within the scatter of data from the related studies of Le Breton and Thompson (1988) and Carrington and Harley (1995) (Fig. 7).

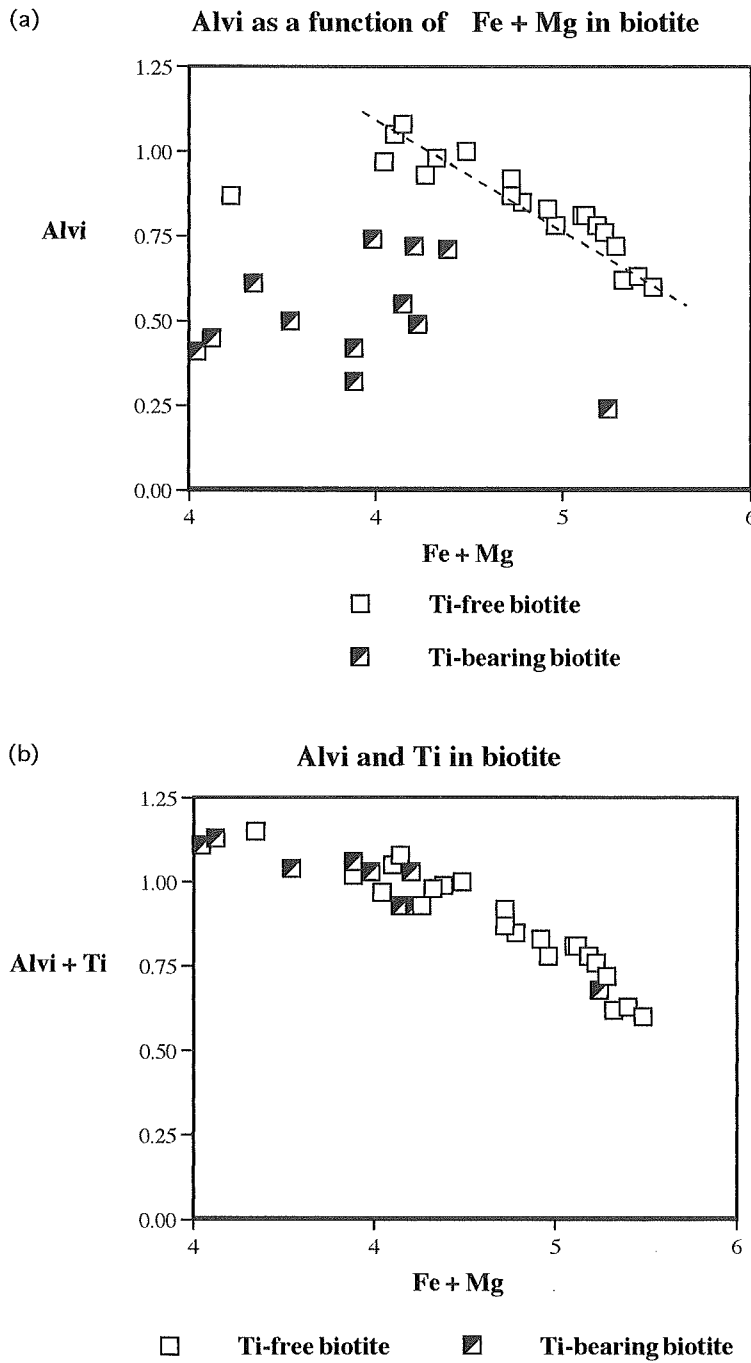


Figure 5: (a) $Al(6)$ plotted against $Mg + Fe$ in biotite produced in this study. The data for the Ti-free, synthetic biotites define a linear trend that is consistent with the substitution $0.66Al + 0.33\square = (Fe,Mg)$. The data for the Ti-bearing biotites plot off this trend. (b) If Ti is added to $Al(6)$ the data for the Ti-bearing biotites define a trend consistent with the substitution $0.5Ti + 0.66Al + 0.85\square = 2(Fe,Mg)$. This necessitates a constant ratio of Ti to $Al(6)$ of 0.75:1.

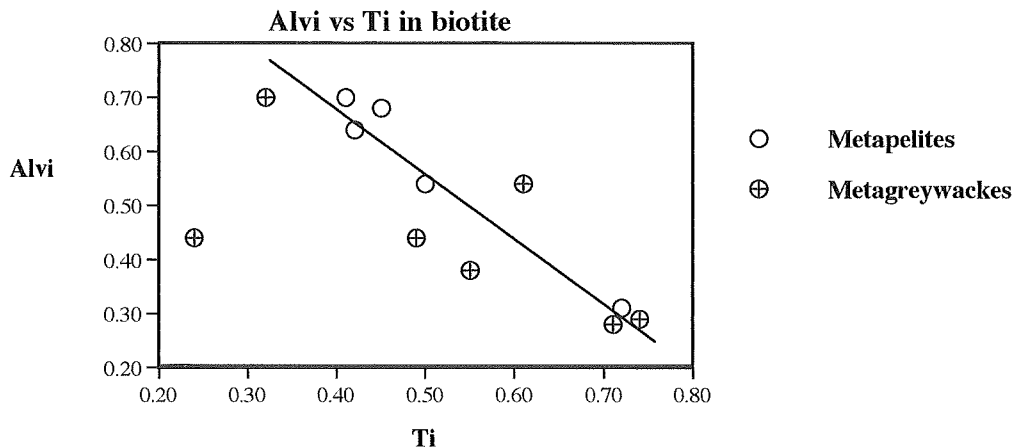


Figure 6: Ti plotted against octahedral Al for the Ti -bearing biotites in both the metapelite and metagreywacke, confirming that the ratio of Ti to $Al(6)$ approximates to 0.75:1. The trend through the data was drawn in by optical best fit.

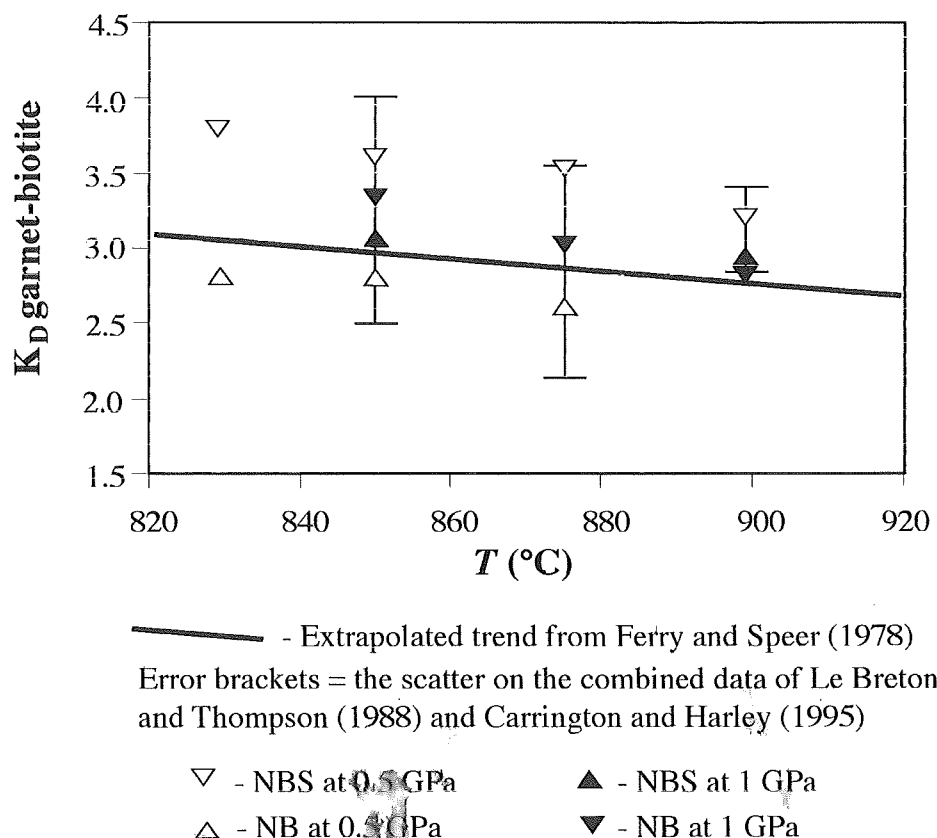


Figure 7: Plot of garnet-biotite KD versus temperature for bulk-compositions NB and NBS, at both 0.5 and 1 GPa. The data define generally linear trends that are subparallel to the extrapolated trend of the Ferry and Spear (1978) geothermometer. The brackets are the combined scatter on the published data of Le Breton and Thompson (1988) and Carrington and Harley (1995).

Garnet

The garnet compositions fall within the almandine - pyrope solid solution series and the crystals always contain less than 10% grossular. Mn content is close to zero in all cases. The compositions of garnets in metagreywacke and metapelite samples at the same pressure are very similar (Fig. 8a to d). Within either compositional group, increasing bulk-rock Mg# results in more Mg-rich garnet compositions, as does increasing temperature. For any bulk-rock Mg#, garnets produced in experiments at 0.5 GPa are substantially more Fe-rich than those produced at 1 GPa. This is consistent with the systematics of the two divariant equilibria controlling garnet composition in metasediments at granulite grade i.e. $\text{Grt} + \text{Qtz} + \text{Sil} = \text{Crd}$, and $\text{Grt} + \text{Qtz} = \text{Crd} + \text{Opx}$, in metapelites and metagreywackes respectively (Hensen, 1971; Hensen and Green, 1972).

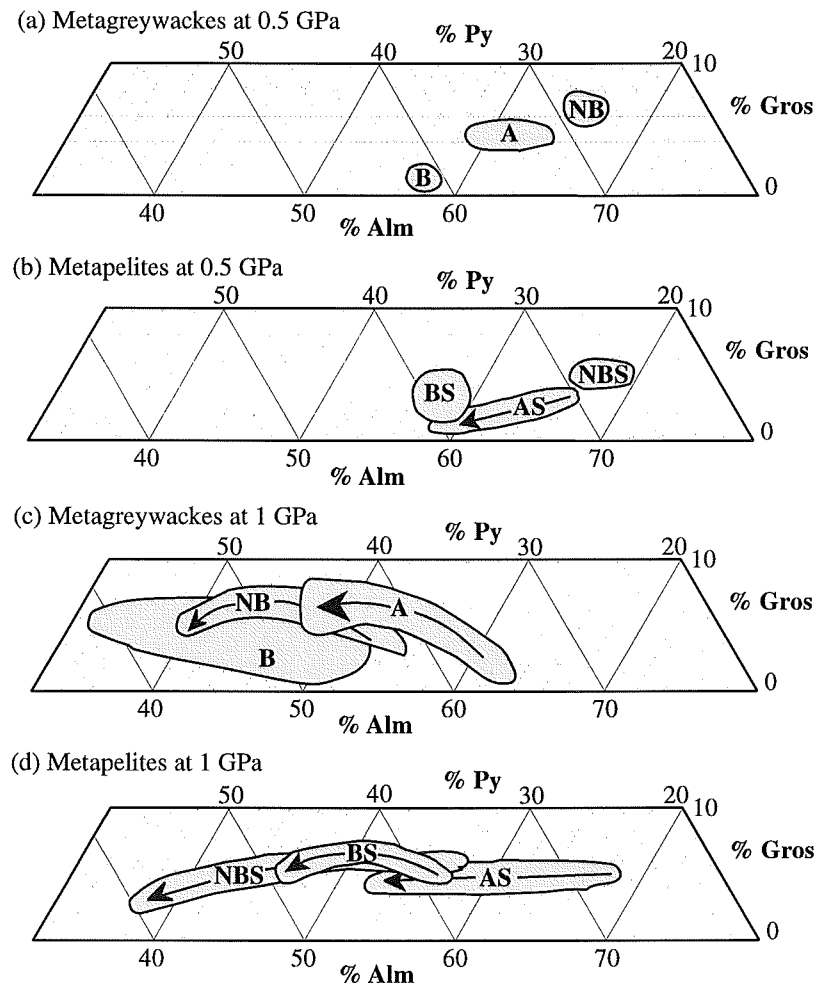
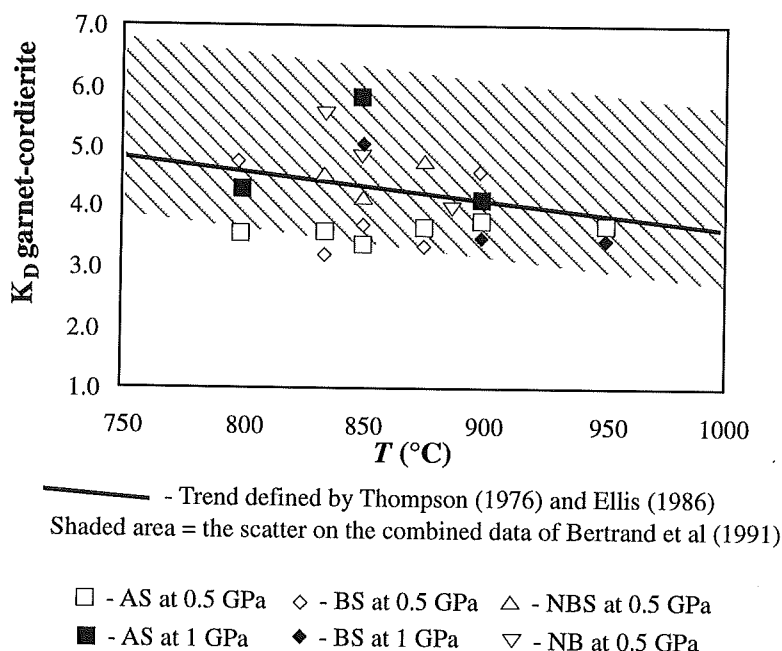


Figure 8: Garnet compositions produced in the experiments plotted according to grossular, almandine and pyrope proportions. (a & b) Garnet compositions produced in the metapelites and metagreywackes respectively, at 0.5 GPa. (c & d) Garnet compositions produced in the metapelites and metagreywackes respectively, at 1 GPa.

Cordierite, Orthopyroxene and Spinel

Cordierite cation totals are generally above the ideal of 11 for a cordierite formula calculated on the basis of 18 oxygens. The degree to which the total exceeds 11 is largely a function of the K content of the cordierite. This suggests that K is not chemically bound into the cordierite framework, but occurs in the channelways in the mineral structure, as suggested by Vry *et al.* (1990). These authors further proposed that the K-cation is charge balanced by volatile species also accommodated in the channelways. Apart from the alkali content, the cordierite compositions are close to ideal and the only notable variations involve Fe - Mg exchange. In the run products, where garnet and cordierite coexisted, Fe-Mg partitioning has been compared to that predicted by the garnet-cordierite thermometer of Thompson (1976) and the results of two relevant phase equilibrium studies by Hensen and Green (1973) and Bertrand *et al.* (1991). Almost without exception, the present data fall within the range defined by these previous studies (fig. 9). In combination with the garnet-biotite Fe-Mg partitioning and the lack of disequilibrium textural evidence this is taken to indicate an acceptable approach to equilibrium in the experiments.



*Figure 9: Plot of garnet-cordierite KD versus temperature for all samples where garnet and cordierite coexisted. The solid line represents the trend of the Thompson (1976) garnet-cordierite thermometer. The shaded area represents the 1000 °C scatter of the data of Bertrand *et al.* (1991) and Hensen and Green (1972), extrapolated to lower temperature, where equilibration of their charges would presumably have been worse.*

The orthopyroxene analyses are generally characterised by high, but variable, Al_2O_3 concentrations. The amount of excess Al_2O_3 in orthopyroxene produced in these experiments appears to be a function of $a\text{Al}_2\text{O}_3$, with orthopyroxene in the metapelites at both 0.5 and 1 GPa

containing more Al_2O_3 than the equivalent metagreywackes. The pressure control on Al_2O_3 in orthopyroxene, calibrated by Harley (1984), is not discernible from the present data. The only significant variations in orthopyroxene composition result from Fe-Mg exchange.

Spinel in the metapelite run products contains significant, but minor, Fe^{3+} (calculated from the $\text{Fe} + \text{Mg}$ excess over $\text{Fe} + \text{Mg} : \text{Al} = 1:2$), indicating solid-solution between hercynite (FeAl_2O_4) and magnetite (Fe_3O_4). This system has been investigated experimentally and the solid-solution has been found to be complete above 858 °C (Turnock and Eugster, 1962). The Mg-component (MgAl_2O_4) is limited but increases with increasing temperature. The magnetite component decreases with increasing temperature.

Glass (Quenched Melts)

The composition of melts produced from the anatexis of metapelites and metagreywackes should be granitic due to the dominant quartz-feldspar-water equilibria that control melting. For anatexis occurring through the incongruent melting of muscovite and biotite, this will even be the case for sources that initially contain no K-feldspar (Winkler, 1976; Green, 1976). The liquids produced should also be saturated in the coexisting AFM restitic assemblage. As the degree of melting increases, the glass compositions should evolve towards that of the coexisting restite. Representative glass analyses and CIPW norms are presented in Table 5a to d and generally reflect the predicted trends. The initial melt compositions produced in the Ti-free metagreywackes and metapelites are very similar, as are those in the Ti-bearing metagreywacke and metapelite (Table 5). In the 6 Ti-free compositions this results from buffering of the melt composition by quartz, plagioclase and K-feldspar. All the glasses have a high and restricted range of SiO_2 contents from ~76% to ~72 % and there is a definite negative correlation between SiO_2 content and temperature (Fig. 10). All the glasses are peraluminous and could generally be classified as having S-type characteristics (Chappel and White, 1974) (Fig. 11). Melts equilibrated with aluminous, granulite-grade, AFM assemblages should be strongly peraluminous. Thompson and Tracy (1977) and Clemens and Wall (1981) predicted a normative corundum value of 5 wt%. Data from this study indicate a value of between 2 and 3 wt%. Corundum content increases slightly with increasing temperature. Normative hypersthene contents of the glasses increase strongly with increasing temperature (Fig. 12). In both the metapelite and metagreywacke groups there is an inverse correlation between bulk-rock Mg# and total $\text{FeO} + \text{MgO}$ in the glass. At both 0.5 and 1 GPa, glasses produced below 900 °C are sufficiently K_2O -rich, relative to SiO_2 , to be considered of alkaline affinity. (Fig. 13). At temperatures in excess of 900 °C total alkalies fall, relative to silica, resulting in compositions that could be classified as calc-alkaline.

The glass compositions produced in this study give a useful indication of the original major element composition of granitic magmas produced through biotite breakdown in metasediments during granulite grade metamorphism. The majority of natural granitic rocks contain some Ti-rich phase and are probably derived from Ti-bearing source rocks. Thus, the glass compositions

produced in samples Nb and NBS probably best reflect the original compositions of natural granites derived from similar source rocks. At 1.0 GPa these glasses are characterised by the following trends with increasing temperature. The K_2O content of the melts decreases, but the presence of biotite in the residual assemblage seems to buffer melt K_2O contents to > 5 wt%. Na_2O content decreases and CaO increases. Normative hypersthene and Mg# both increase. The SiO_2 contents of the glasses are high (ranging from 73.38 to 74.71 wt%), consistent with the fact that most of the experiments remained quartz-saturated.

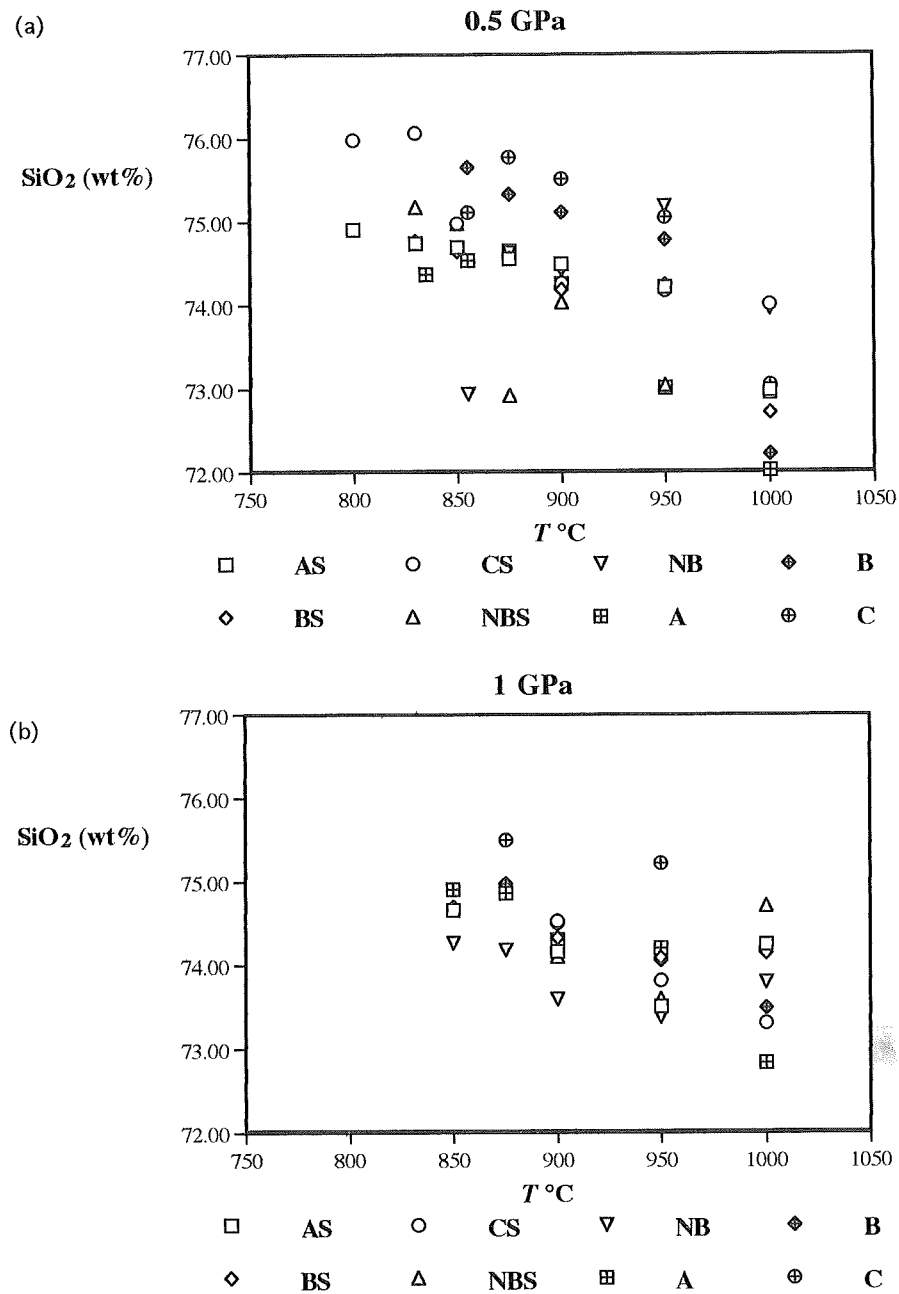


Figure 10: SiO_2 contents of the glasses versus temperature, (a) at 0.5 GPa, (b) at 1.0 GPa.

Table 5a: Glass compositions from the metapelites at 0.5 Gpa

	AS	AS	AS	AS	AS	AS	BS							
T°C	800	830	850	875	900	950	1000	800	830	850	875	900	950	1000
SiO₂	74.91	74.74	74.69	74.69	74.49	74.21	72.98	74.93	74.77	74.64	74.63	74.25	74.24	73.05
Al₂O₃	14.57	14.54	14.34	14.19	14.29	14.36	14.51	14.53	14.04	14.35	14.26	14.18	14.22	15.00
TiO₂	0.00	0.00	0.00	0.00	0.00	0.00	0.00	0.00	0.00	0.00	0.00	0.00	0.00	0.00
MgO	0.32	0.37	0.37	0.28	0.25	0.40	0.44	0.36	0.58	0.30	0.27	0.48	0.54	0.53
FeO	1.54	1.60	1.66	1.78	1.65	2.67	3.45	1.36	1.64	1.61	1.68	1.78	2.10	2.70
CaO	0.64	0.70	0.69	0.62	0.64	1.02	1.55	0.69	0.70	0.75	0.74	0.63	1.01	1.29
Na₂O	2.31	2.25	2.23	2.46	2.30	2.41	2.53	2.49	2.56	2.34	2.16	2.28	2.14	2.06
K₂O	5.71	5.79	6.02	5.96	6.39	4.93	4.54	5.63	5.72	6.01	6.25	6.39	5.80	5.35
Q	36.48	36.10	35.26	34.23	33.53	36.31	34.02	35.74	34.25	34.62	34.72	32.94	34.87	34.52
Ab	19.55	19.04	18.87	20.82	19.46	20.39	21.41	21.07	21.66	19.80	18.28	19.29	18.11	17.43
An	3.18	3.47	3.42	3.08	3.18	5.06	7.69	3.42	3.47	3.72	3.67	3.13	5.01	6.40
Or	33.74	34.22	35.58	35.16	37.76	29.14	26.83	33.27	33.80	35.52	36.88	37.70	34.28	31.50
C	3.43	3.30	2.90	2.55	2.43	3.20	2.62	3.09	2.36	2.63	2.60	2.37	2.59	3.43
Hy	3.62	3.86	3.97	3.97	3.65	5.90	7.43	3.39	4.46	3.70	3.76	4.46	5.20	6.28
Il	0.00	0.00	0.00	0.00	0.00	0.00	0.00	0.00	0.00	0.00	0.00	0.00	0.00	0.00
Mg#	0.27	0.29	0.28	0.22	0.21	0.21	0.19	0.32	0.39	0.25	0.22	0.33	0.31	0.26

	CS	NBS	NBS	NBS	NBS	NBS	NBS	NBS						
T°C	800	830	850	875	900	950	1000	830	850	875	900	950	1000	
SiO₂	75.98	76.35	74.98	74.71	74.26	74.92	74.01	75.17	74.98	72.92	74.03	73.04	72.95	
Al₂O₃	13.78	13.30	14.07	14.34	14.45	14.41	14.58	14.03	14.07	15.17	14.32	14.67	14.54	
TiO₂	0.00	0.00	0.00	0.00	0.00	0.00	0.00	0.20	0.37	0.42	0.46	0.58	0.59	
MgO	0.18	0.21	0.37	0.40	0.41	0.63	0.56	0.19	0.24	0.73	0.73	0.82	0.97	
FeO	0.89	0.90	1.30	1.28	1.30	1.61	2.10	1.28	1.50	1.78	1.62	1.91	2.05	
CaO	0.69	0.74	0.76	0.73	0.74	1.06	1.26	0.59	0.69	0.80	0.82	1.04	1.32	
Na₂O	2.51	2.49	2.37	2.22	2.16	1.96	2.14	2.89	2.71	2.68	2.58	2.47	2.23	
K₂O	5.96	6.00	6.15	6.32	6.68	5.41	5.35	5.66	5.43	5.52	5.43	5.46	5.34	
Q	36.08	36.09	34.39	34.25	32.84	37.87	35.79	34.23	35.62	32.23	34.38	33.16	33.99	
Ab	21.24	20.99	20.06	18.79	18.28	16.42	18.11	24.46	22.93	22.68	21.83	20.90	18.87	
An	3.42	3.67	3.77	3.62	3.67	5.21	6.25	2.93	3.42	3.97	4.07	5.16	6.55	
Or	35.22	35.34	36.34	37.29	39.48	31.68	31.62	33.45	32.09	32.62	32.09	32.27	31.56	
C	1.95	1.35	2.13	2.50	2.32	3.37	2.98	2.08	2.48	3.33	2.71	2.81	2.69	
Hy	2.08	2.18	3.31	3.35	3.41	4.46	5.25	2.49	2.74	4.39	4.03	4.59	5.21	
Il	0.00	0.00	0.00	0.00	0.00	0.00	0.00	0.38	0.70	0.80	0.87	1.10	1.12	
Mg#	0.26	0.30	0.33	0.36	0.36	0.41	0.32	0.21	0.22	0.42	0.44	0.43	0.46	

Table 5b: Glass compositions from the metagreywackes at 0.5 Gpa

	A	A	A	A	A	A	B	B	B	B	B	C	C	C
T°C	835	855	875	900	950	1000	855	875	900	950	1000	855	875	900
SiO₂	74.37	74.53	74.65	74.25	73.01	72.02	75.65	75.33	75.11	74.78	72.22	75.11	75.77	75.51
Al₂O₃	13.26	13.40	13.57	13.94	14.79	14.84	13.53	13.27	13.35	13.44	15.10	13.04	12.95	13.09
TiO₂	0.00	0.00	0.00	0.00	0.00	0.00	0.00	0.00	0.00	0.00	0.00	0.00	0.00	0.00
MgO	1.17	0.95	0.39	0.52	0.72	0.81	0.44	0.52	0.57	0.79	0.89	2.07	0.85	1.12
FeO	2.86	2.18	1.88	1.76	2.89	3.73	1.11	1.67	1.96	1.86	2.39	0.96	1.10	1.08
CaO	0.70	0.87	0.85	1.09	1.35	1.59	0.77	0.87	0.93	1.07	1.40	0.67	0.88	0.92
Na₂O	2.23	2.24	2.46	2.31	2.24	2.21	2.33	2.01	1.96	1.73	2.48	2.17	2.19	2.06
K₂O	5.41	5.83	6.22	6.13	4.99	4.79	6.17	6.33	6.12	6.33	5.51	5.97	6.25	6.21
Q	35.06	34.08	32.56	32.77	34.50	33.10	35.25	35.37	35.80	35.46	30.38	34.31	35.04	35.21
Ab	18.87	18.96	20.82	19.55	18.96	18.70	19.72	17.01	16.59	14.64	20.99	18.36	18.53	17.43
An	3.47	4.32	4.22	5.41	6.70	7.89	3.82	4.32	4.61	5.31	6.95	3.32	4.37	4.56
Or	31.97	34.45	36.76	36.23	29.49	28.31	36.46	37.41	36.17	37.41	32.56	35.28	36.94	36.70
C	2.46	1.82	1.25	1.52	3.25	3.13	1.62	1.53	1.81	1.80	2.51	1.79	0.98	1.31
Hy	8.17	6.37	4.42	4.53	7.10	8.87	3.13	4.36	5.02	5.38	6.61	6.92	4.14	4.77
Il	0.00	0.00	0.00	0.00	0.00	0.00	0.00	0.00	0.00	0.00	0.00	0.00	0.00	0.00
Mg#	0.42	0.44	0.27	0.35	0.31	0.28	0.41	0.36	0.34	0.43	0.40	0.79	0.58	0.65

	C	C	NB	NB	NB	NB	NB
T°C	950	1000	855	875	900	950	1000
SiO₂	75.05	73.05	73.01	74.63	74.42	75.18	73.96
Al₂O₃	13.24	14.60	14.60	14.45	14.31	13.33	14.56
TiO₂	0.00	0.00	0.70	0.24	0.57	0.73	0.60
MgO	1.32	1.49	1.02	0.45	0.63	0.58	1.09
FeO	1.29	1.77	1.79	1.75	2.16	2.24	2.47
CaO	1.18	1.40	0.89	0.99	0.94	1.66	1.29
Na₂O	1.75	2.18	2.77	2.58	2.23	1.94	2.69
K₂O	6.16	5.51	5.20	4.91	4.75	4.35	3.34
Q	35.72	32.58	32.53	36.75	38.94	41.50	39.52
Ab	14.81	18.45	23.44	21.83	18.87	16.42	22.76
An	5.85	6.95	4.42	4.91	4.66	8.24	6.40
Or	36.40	32.56	30.73	29.02	28.07	25.71	19.74
C	1.55	2.50	2.79	3.09	3.79	2.41	4.17
Hy	5.66	6.96	4.67	3.94	4.59	4.35	6.26
Il	0.00	0.00	1.33	0.46	1.08	1.39	1.14
Mg#	0.65	0.60	0.50	0.32	0.34	0.31	0.44

Table 5c: Glass compositions from the metapelites at 1 Gpa.

T°C	AS 850	AS 900	AS 950	AS 1000	BS 850	BS 900	BS 950	BS 1000	CS 900	CS 950	CS 1000	NBS 900	NBS 950	NBS 1000
SiO₂	74.66	74.17	73.64	74.25	74.70	74.33	74.09	74.15	74.24	73.82	73.31	74.11	73.60	74.71
Al₂O₃	14.41	14.37	14.86	14.86	14.53	14.64	14.15	14.83	14.30	14.41	14.78	14.75	15.19	14.80
TiO₂	0.00	0.00	0.00	0.00	0.00	0.00	0.00	0.00	0.00	0.00	0.00	0.39	0.76	0.69
MgO	0.46	0.45	0.48	1.26	0.53	1.07	0.78	1.23	0.76	0.99	1.22	0.71	1.21	1.64
FeO	1.45	1.50	1.24	1.57	1.23	0.98	1.46	1.69	1.15	1.04	1.18	1.20	1.07	0.96
CaO	0.64	0.68	0.74	1.20	0.64	0.81	1.01	1.22	0.67	1.25	1.54	0.97	1.75	1.54
Na₂O	2.44	2.52	2.90	2.34	2.44	2.29	2.22	2.32	2.41	2.14	1.95	2.66	2.14	1.95
K₂O	5.94	6.31	6.14	4.52	5.94	5.88	6.28	4.55	6.46	6.35	6.02	5.21	4.29	3.71
Q	34.46	31.98	29.90	37.57	34.58	34.35	32.59	37.38	32.08	32.04	32.82	34.85	38.85	43.14
Ab	20.65	21.32	24.46	19.80	20.65	19.38	18.79	19.63	20.48	18.11	16.50	22.51	18.11	16.50
An	3.18	3.37	3.67	5.95	3.18	4.02	5.01	6.05	3.32	6.20	7.64	4.81	8.68	7.64
Or	35.10	37.29	36.23	26.71	35.10	34.75	37.11	26.89	38.35	37.53	35.58	30.79	25.35	21.93
C	2.80	2.16	2.10	3.94	2.92	3.04	1.86	3.87	2.14	1.74	2.26	2.97	3.84	4.78
Hy	3.81	3.88	3.47	6.02	3.58	4.46	4.62	6.17	4.00	4.38	5.21	3.33	3.72	4.71
Il	0.00	0.00	0.00	0.00	0.00	0.00	0.00	0.00	0.00	0.00	0.00	0.74	1.44	1.31
Mg#	0.36	0.35	0.41	0.59	0.43	0.66	0.49	0.56	0.54	0.63	0.65	0.51	0.67	0.75

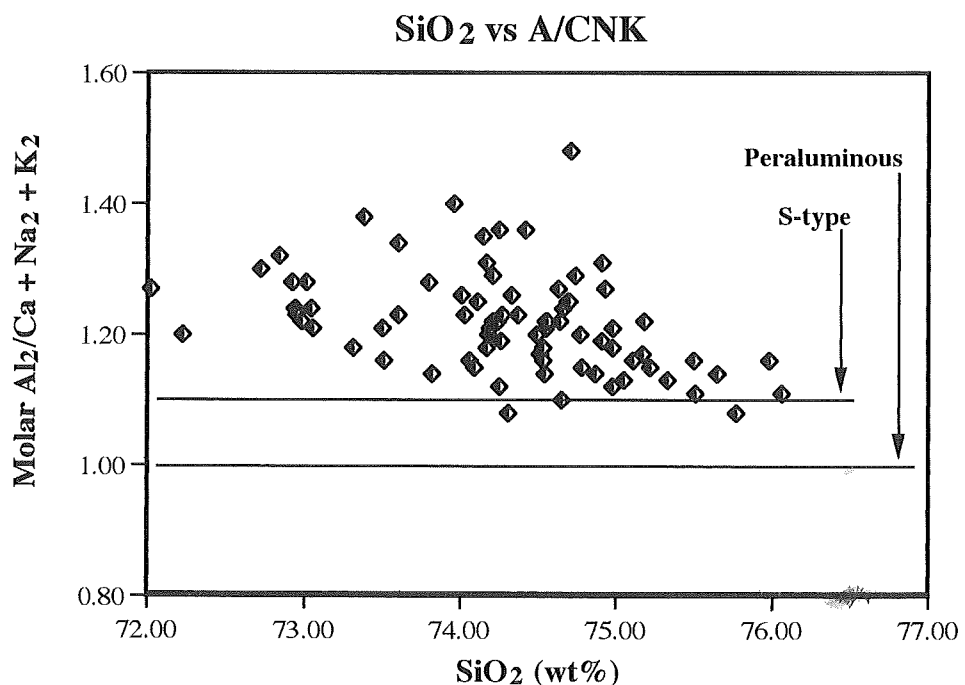


Figure 11: Plot of SiO₂ versus A/CNK for all the glass compositions produced in this study. The trend of decreasing SiO₂ content and increasing A/CNK generally correlates with increasing temperature.

Table 5d: Glass compositions from the metagreywackes at 1 Gpa

	A	A	A	A	A	B	B	B	B	C	C	C	NB	
T°C	850	875	900	950	1000	875	900	950	1000	875	900	950	1000	850
SiO₂	74.91	74.87	74.31	74.21	72.84	74.98	74.54	74.10	73.50	75.50	74.51	75.22	73.75	74.27
Al₂O₃	14.00	13.83	13.63	14.28	15.40	13.79	14.01	14.33	14.73	14.19	14.62	13.70	14.86	14.38
TiO₂	0.00	0.00	0.00	0.00	0.00	0.00	0.00	0.00	0.00	0.00	0.00	0.00	0.00	0.39
MgO	0.44	0.51	0.66	1.04	1.29	0.44	0.43	0.47	0.66	0.31	0.51	0.79	0.52	0.49
FeO	1.57	1.49	1.86	1.73	1.97	1.43	1.60	1.69	1.86	0.63	0.83	1.00	0.99	1.62
CaO	0.74	0.95	1.02	1.18	1.51	1.08	1.12	1.15	1.36	1.05	1.07	1.01	1.36	0.95
Na₂O	2.49	2.43	2.64	2.46	2.32	2.41	2.17	2.22	2.16	2.39	2.48	2.01	2.46	2.43
K₂O	5.85	5.92	5.87	5.10	4.68	5.87	6.13	6.09	5.72	5.93	5.98	6.28	6.07	5.47
Q	34.48	34.03	31.76	34.85	34.63	34.33	34.08	33.30	33.59	35.66	33.45	35.31	31.69	35.37
Ab	21.07	20.56	22.34	20.82	19.63	20.39	18.36	18.79	18.28	20.22	20.99	17.01	20.82	20.56
An	3.67	4.71	5.06	5.85	7.49	5.36	5.56	5.71	6.75	5.21	5.31	5.01	6.75	4.71
Or	34.57	34.99	34.69	30.14	27.66	34.69	36.23	35.99	33.80	35.04	35.34	37.11	35.87	32.33
C	2.23	1.70	1.08	2.57	3.77	1.51	1.77	2.00	2.51	1.93	2.12	1.76	1.77	2.73
Hy	3.98	4.01	5.06	5.77	6.83	3.72	4.01	4.27	5.06	1.93	2.79	3.80	3.11	3.55
Il	0.00	0.00	0.00	0.00	0.00	0.00	0.00	0.00	0.00	0.00	0.00	0.00	0.00	0.74
Mg#	0.33	0.38	0.39	0.52	0.54	0.36	0.32	0.33	0.39	0.47	0.52	0.58	0.48	0.35

	NB	NB	NB	NB
T°C	875	900	950	1000
SiO₂	74.19	73.60	73.38	73.80
Al₂O₃	14.44	14.54	15.15	14.88
TiO₂	0.50	0.46	0.53	0.60
MgO	0.48	0.73	1.28	1.13
FeO	1.39	1.87	1.71	1.11
CaO	1.02	1.06	1.43	1.56
Na₂O	2.63	2.64	2.37	2.41
K₂O	5.35	5.11	4.17	4.50
Q	34.73	34.11	37.63	37.05
Ab	22.26	22.34	20.06	20.39
An	5.06	5.26	7.09	7.74
Or	31.62	30.20	24.64	26.59
C	2.47	2.74	4.14	3.21
Hy	2.92	4.49	5.45	3.86
Il	0.95	0.87	1.01	1.14
Mg#	0.38	0.41	0.57	0.64

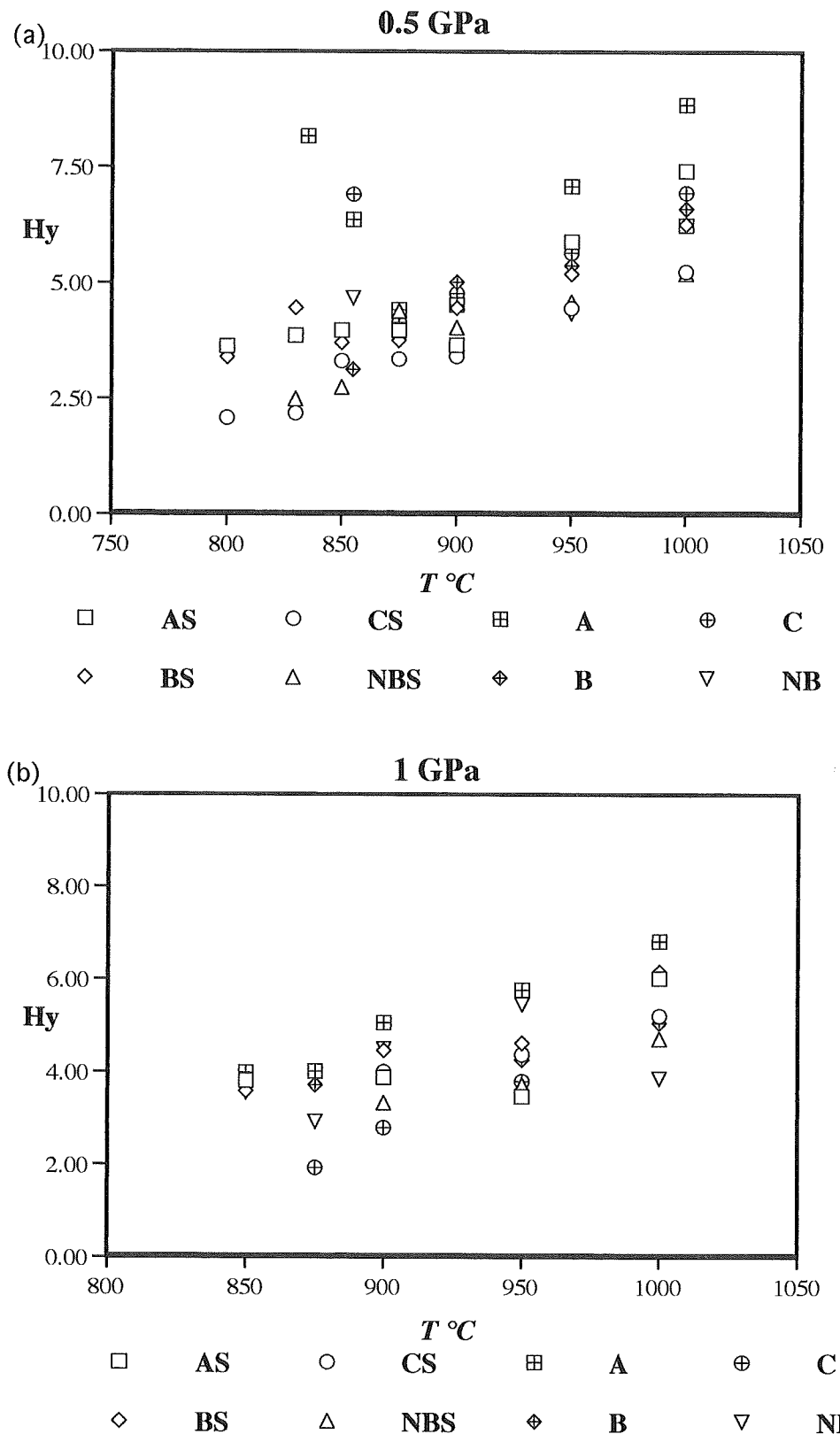


Figure 12: Normative hyperssthene contents of the glasses versus temperature, (a) at 0.5 GPa, (b) at 1.0 GPa.

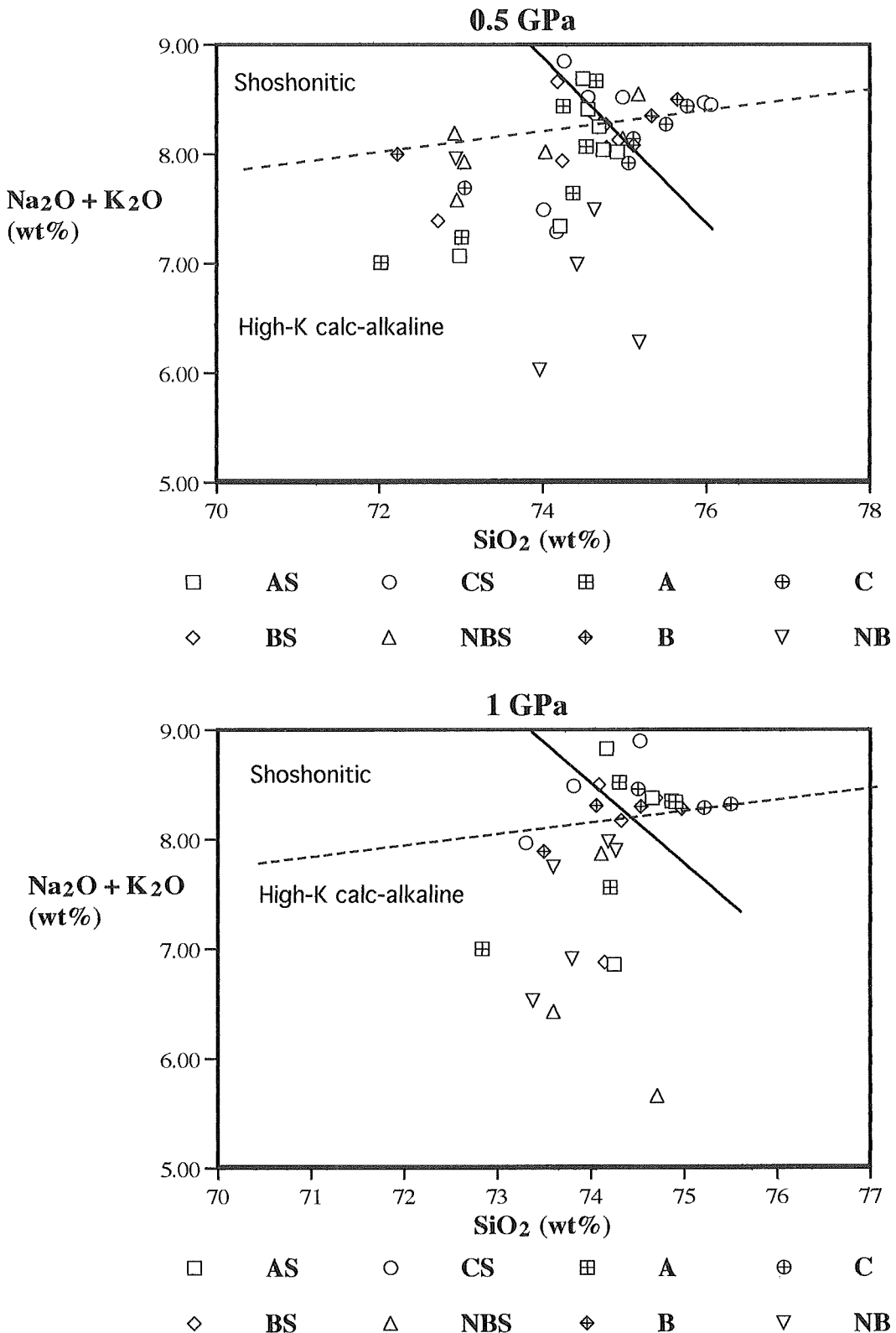


Figure 13: K_2O versus SiO_2 for glasses from 0.5 GPa (a) and 1 GPa (b). The dashed lines divide high SiO_2 , high total alkali, compositions produced at $T < 900^\circ\text{C}$, from more typical compositions of calc-alkaline affinity produced at higher temperatures. The high-K calc-alkaline - shoshonitic field boundary is from Rickwood (1989).

SOURCE-ROCK FERTILITY

Phase proportions in all the hypersolidus run products were determined for experiments at 800, 850, 900, 950 and 1000 °C by a combination of image analysis on back-scattered electron SEM images and a least squares mixing routine. In the near-solidus runs, cordierite, quartz, plagioclase and K-feldspar are commonly abundant. The grey-scale variations between these phases in the BSE images was insufficient to allow image analysis to be used in estimating the modal proportions. In contrast, garnet, orthopyroxene and biotite showed stark grey-scale variations and the modal proportions of these phases could be determined reliably by this method. Averages of garnet, orthopyroxene and biotite proportions were calculated for 3 representative images from each set of run products. These data were used to "anchor" the least squares mixing calculations that were employed to calculate the modal proportions of all the phases. This methodology optimises both techniques, and total errors on the modal proportion data are believed to be $\leq 3\%$. Variations in phase proportions with temperature, for all eight bulk-compositions, are illustrated in Figures 14 and 15.

The data from this study suggest that, in the case of Ti-free biotites, a significant pulse of melt production is achieved with only slight increases in temperature. The slopes of the melt productivity lines in Figures 14 and 15 are partly dependent on the temperature interval of the experiments. However, in metagreywacke B in particular, the experiments fortuitously bracketed the bulk of melt production (from ~ 5 wt% to > 40 wt%) within a temperature interval of 15 °C. The pattern of melt production in the other compositions is probably similar, but masked by the broader temperature spacing of experiments. In contrast to this behaviour, the Ti bearing biotites break down over an extended temperature range. Particularly at 1 GPa, the Ti-bearing compositions contain significantly less melt than any of the Ti-free samples over the critical temperature range of 800 to 900 °C. This effect is partially masked in the 0.5 GPa runs by the fact that significant discrepancies in melt proportion are present above the biotite out temperature. This has been shown to reflect different proportions of hydrous cordierite in these samples (Stevens *et al.*, 1995). Thus, where cordierite is a dominant product of biotite melting melt fractions are markedly restricted. This is most obvious in the lower pressure experiments where cordierite proportions are maximised (Fig. 14a).

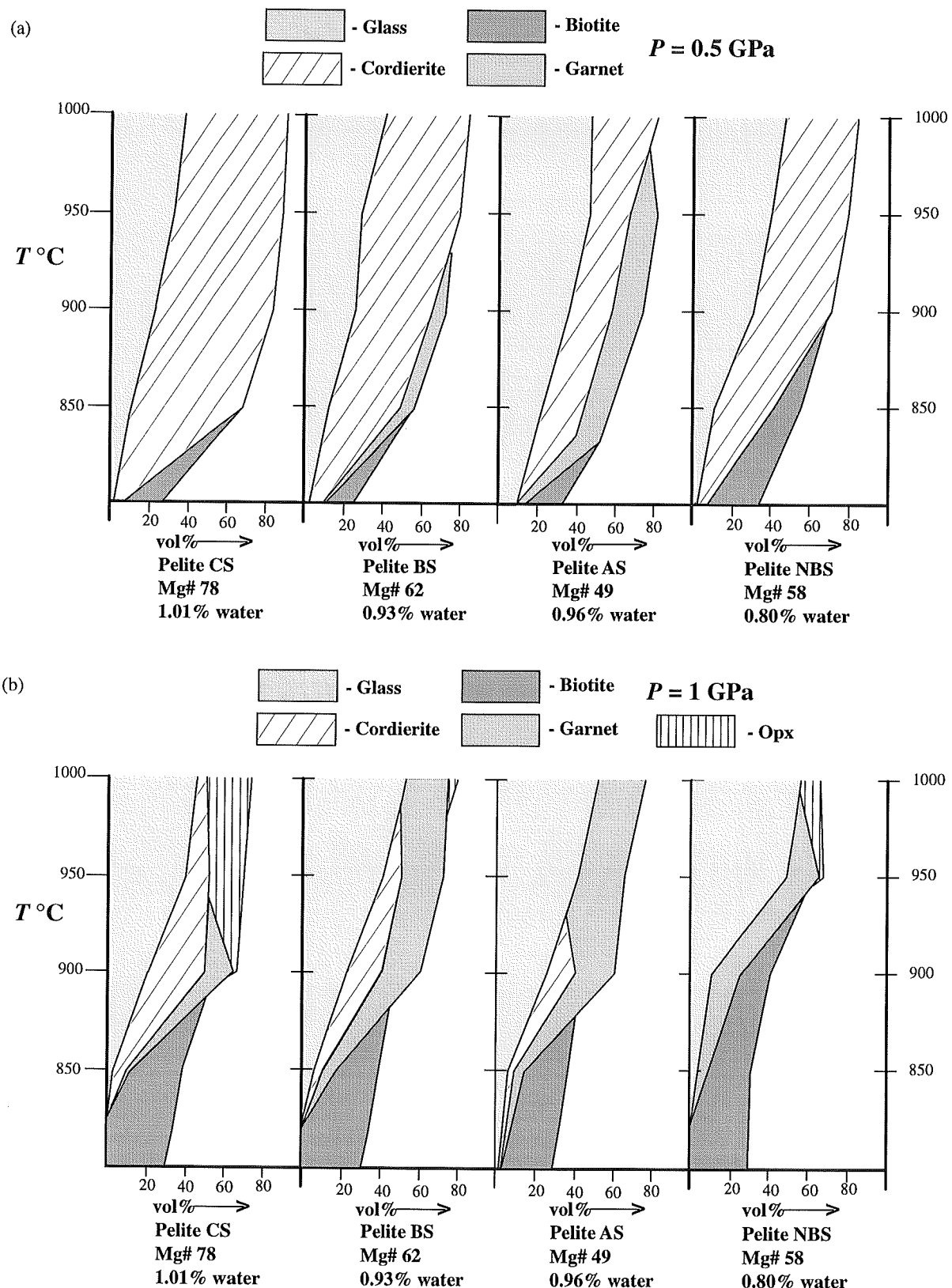


Figure 14: Calculated modal proportions of the major product phases and biotite in the metapelite run products, (a) at 0.5 GPa, (b) at 1.0 GPa.

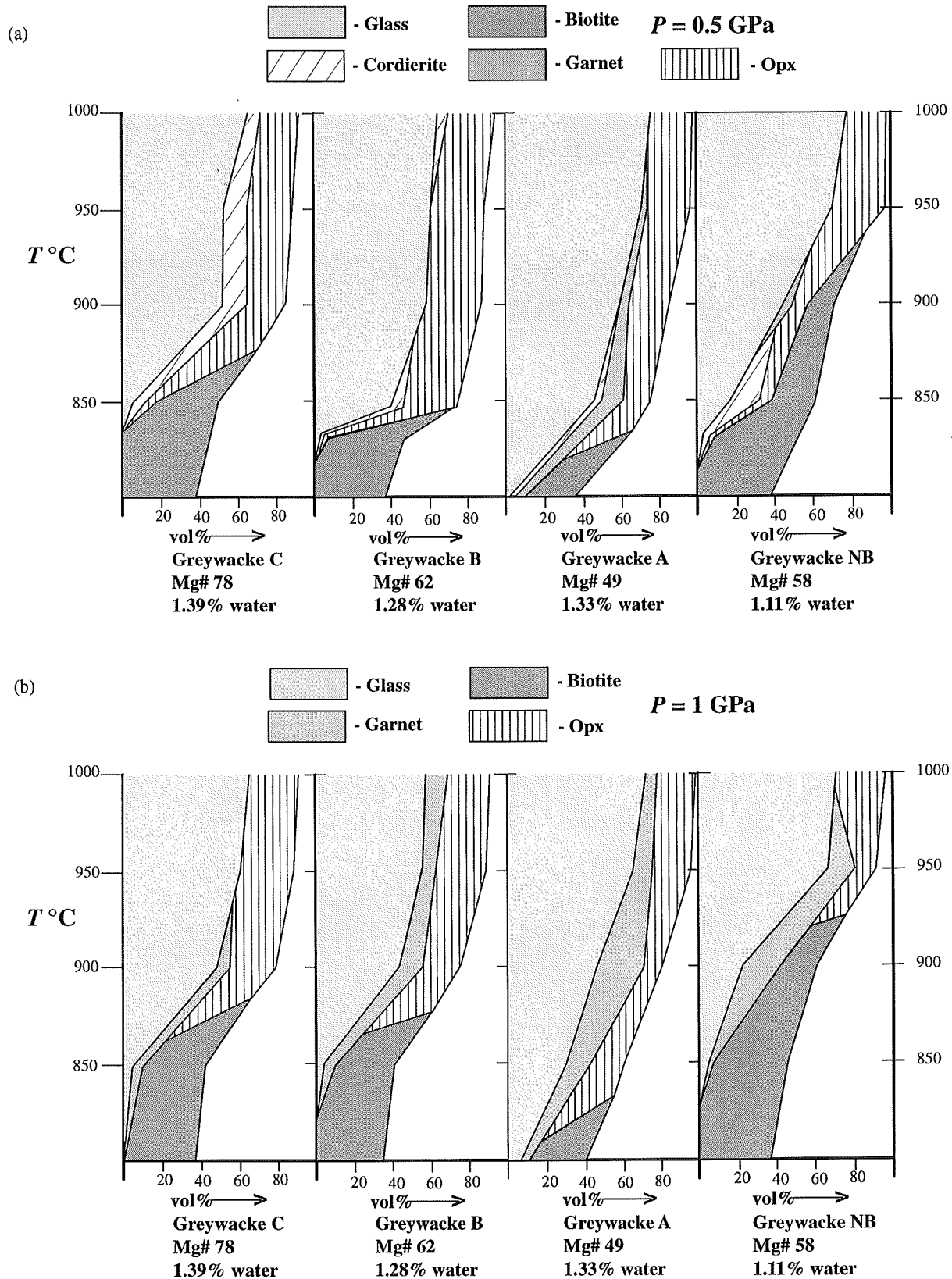


Figure 15: Calculated modal proportions of the major product phases and biotite in the metagreywacke run products, (a) at 0.5 GPa, (b) at 1.0 GPa.

CONCLUSIONS

This work has followed on that of many others (Brown and Fyfe, 1970; Huang and Wyllie, 1981; Vielzeuf and Holloway, 1988; Patiño-Douce and Johnston, 1991; Vielzeuf and Montel, 1994) in confirming the viability of producing crustally derived granitic magma, with the right characteristics for intrusion of the upper crust, from metasedimentary sources during fluid-absent granulite-grade metamorphic episodes. During such fluid-absent anatetic episodes the fertility of metapelites and metagreywackes, with "normal" quartz and plagioclase contents, is determined by the behaviour of both biotite and cordierite. Biotite is the H₂O-reservoir in the pre-melting assemblage. Thus, every increment of biotite breakdown produces an increment of melt production (the amount of melt is controlled by the H₂O solubility in the melt which is a function of pressure). This study shows that in reduced metapelite and metagreywacke granulites, Mg# and Ti-content are the bulk-rock compositional variables most likely to control fluid-absent biotite melting (Fig. 16). In Ti-free compositions large pulses of melt production occur between 800 to 875 °C as a function of increasing bulk-rock Mg#. In relatively Fe-rich samples melt fractions in excess of 40 % can be attained at temperatures less than 850 °C. With the inclusion of a Ti component, biotite is stabilised to temperatures between 900 and 950 °C. In consequence, in titaniferous compositions temperature must approximate 950 °C before melt fractions exceed 40 %. The cordierite produced by fluid-absent biotite melting is hydrous. Where the modal proportions of cordierite are high (a function of bulk-rock Mg#, α Al₂O₃ and pressure) melt production is severely restricted. In these rocks cordierite represents a H₂O reservoir that cannot be tapped by melting reactions during metamorphism of the mid-crust, because in this environment, cordierite is stable to temperatures in excess of 1000 °C. The glass compositions (quenched melt) produced in this study cluster very tightly. In general the glasses have very similar compositions to those of natural strongly peraluminous leucogranites that are believed to represent close to original melt compositions and should prove useful in providing constraints on the original magma compositions during studies modelling the evolution of such magmas. The range of bulk compositional variables investigated in this study had only a minor influence on the temperature of first melting. All suitable metasedimentary granulites metamorphosed to 830 °C should contain evidence of anatexis if fluid-absent conditions prevailed during the peak of metamorphism. If the reactions described in this study can be recognised in natural rocks Figure 1 can be used as a useful geothermometer.

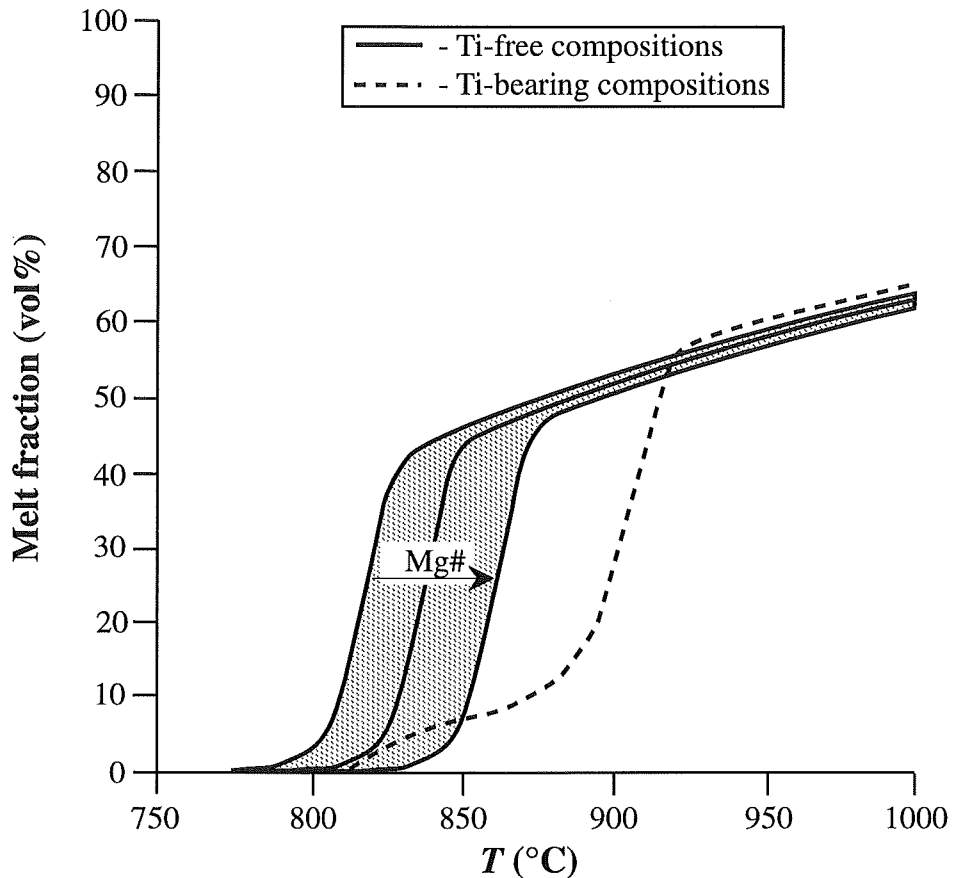


Figure 16: Model of fluid-absent melting behaviour in both Ti-bearing and Ti-free metagreywackes, with variable Mg#. The bulk-rock contains ~ 1.25 wt% H_2O , and cordierite is not a major product of biotite breakdown.

ABBREVIATIONS

Ab albite; An anorthite; Bt biotite; Crd cordierite; Gl glass; Grt garnet; Il ilmenite; Kfs K-feldspar; Opx orthopyroxene; Or orthoclase; Pl plagioclase; Qtz quartz; Ru rutile; Sp spinel.

ACKNOWLEDGEMENTS

The authors are grateful to the Natural and Environmental Research Council for support through research grant GR3/8215 to J.D.C. and G.T.R.D.

REFERENCES

- Ashwal, L.D., Morgan, P. and Hoisch, T.D., 1992, Tectonics and heat sources for granulite metamorphism of supracrustal-bearing terranes. *Precambrian Research*, v. 55, p.525-538.
- Bertrand, P., Ellis, D.J. and Green, D.H., 1991, The stability of sapphirine-quartz and

- hypersthene-sillimanite-quartz assemblages: an experimental investigation in the system FeO-MgO-Al₂O₃-SiO₂ under H₂O and CO₂ conditions. Contributions to Mineralogy and Petrology, v. 108, p. 55-71.
- Brown, G.C. and Fyfe, W.S., 1970, The production of granite melts during ultra-metamorphism. Contributions to Mineralogy and Petrology, v. 240, p. 310-318.
- Carrington, D.P. and Harley, S.L., 1995, Partial melting and phase relations in high-grade metapelites: an experimental petrogenetic grid in the KFMASH system. In press.
- Chappel, B.W. and White, A.J.R., 1974, Two contrasting granite types. Pacific Geology, v. 8, p. 173-174.
- Clemens, J.D. and Wall, V.J., 1981, Crystallisation and origin of some peraluminous (S-type) granitic magmas. Canadian Mineralogist, v. 14, p. 111-132.
- Clemens, J.D. and Vielzeuf, D., 1987, Constraints on melting and magma production in the crust. Earth and Planetary Science Letters, v. 86, p. 287-306.
- Clemens, J.D., 1990, The granulite-granite connexion. In, Vielzeuf, D. and Vidal, Ph. (eds), Granulites and Crustal Evolution, NATO ASI Series, Kluwer Academic Publishers, Dordrecht, 585 p.
- Conrad, W.K., Nicholls, I.A. and Wall, V.J., 1988, Water-saturated and -undersaturated melting of metaluminous and peraluminous crustal compositions at 10 kb: evidence for the origin of silicic magmas in the Taupo volcanic zone, New Zealand, and other occurrences. Journal of Petrology, v. 29, p. 765-803.
- Dymek, R.F., 1983, Titanium, aluminum and interlayer cation substitutions in biotite from high-grade gneisses, West Greenland. American Mineralogist, v. 68, p. 880-899.
- Ellis, D.J., 1986, Garnet-liquid Fe²⁺-Mg equilibria and implications for the beginning of melting in the crust and subduction zones. American Journal of Science, v. 286, p. 765-791.
- Ferry, J.M. and Speer, F.S., 1978, Experimental calibration of the partitioning of Fe and Mg between biotite and garnet. Contributions to Mineralogy and Petrology, v. 66, p. 113-117.
- Fyfe, W.S., 1973, The granulite facies, partial melting and the Archaean crust. Philosophical Transactions of the Royal Society of London, v. A273, p. 457-461.

- Grant, J.A., 1985, Phase equilibria in partial melting of pelitic rocks. In, Ashworth, J.R. (ed), *Migmatites*, Blackie, Glasgow, p. 86-144.
- Green, T.H., 1976, Experimental generation of cordierite- or garnet-bearing granitic liquids from a pelitic composition. *Geology*, v. 4, p. 85-88.
- Guidotti, C.V., 1984, Micas in metamorphic rocks. In, Bailey, S.E. (ed), *Micas*. Mineralogical Society of America, *Reviews in Mineralogy*, v. 13, p. 357-467.
- Harley, S.L., 1984, An experimental study of the partitioning of Fe and Mg between garnet and orthopyroxene. *Contributions to Mineralogy and Petrology*, v. 86, p. 359-373.
- Hensen, B.J., 1971, Theoretical phase relations involving cordierite and garnet in the system $\text{MgO}-\text{FeO}-\text{Al}_2\text{O}_3-\text{SiO}_2$. *Contributions to Mineralogy and Petrology*, v. 33, p. 191-215.
- Hensen, B.J. and Green, D.H., 1972, Experimental study of the stability of cordierite and garnet in pelitic compositions at high pressures and temperatures. II. Compositions without excess alumino-silicate. *Contributions to Mineralogy and Petrology*, v. 35, p. 331-354.
- Hensen, B.J. and Green, D.H., 1973, Experimental study of the stability of cordierite and garnet in pelitic compositions at high pressure and temperature III. Synthesis of experimental data and geological applications. *Contributions to Mineralogy and Petrology*, v. 38, p. 151-166.
- Hoschek, G., 1976, Melting relations of biotite + plagioclase + quartz. *Neues Jahrbuch für Mineralogie Monatshelte*, v. 2, p. 79-83.
- Huang, W.L. and Wyllie, P.J., 1981, Phase relationships of S-type granite with H_2O to 35 kbar: muscovite granite from Harney Peak, South Dakota. *Journal of Geophysical Research*, v. B86, p. 10515-10529.
- Johannes, W. and Holtz, F., 1990, Formation and composition of water-undersaturated granitic melt. In, Ashworth, J.R. and Brown, M. (eds), *High-temperature Metamorphism and Crustal Anatexis*, Unwin Hyman, London, p. 87-104.
- Le Breton, N. and Thompson, A.B., 1988, Fluid-absent (dehydration) melting of biotite in metapelites in the early stages of crustal anatexis. *Contributions to Mineralogy and Petrology*, v. 99, p. 226-237.
- Luth, W.C., 1976, Granitic rocks. In, Bailey, D.K. and MacDonald, R (eds), *The Evolution of Crystalline Rocks*, Academic Press, London, 406 pp.

- Patiño-Douce, A.E. and Johnston, A.D., 1991. Phase equilibria and melt productivity in the pelitic system: implications for the origin of peraluminous granitoids and aluminous granites. Contributions to Mineralogy and Petrology, v. 107, p. 202-218.
- Patiño-Douce, A.E., Johnston, A.D. and Rice, J.M., 1993, Octahedral excess mixing properties in biotite: a working model with applications to geobarometry and geothermometry. American Mineralogist, v. 78, p. 113-131.
- Rickwood, P.C., 1989, Boundary lines within petrologic diagrams which use oxides of major and minor elements. Lithos, v. 22, p. 247-263.
- Rutter, M.J. and Wyllie, P.J., 1987, Melting of tonalite and the origin of crustal granites. EOS, v. 68, p. 441
- Skjerlie, K.P. and Johnston, A.D., 1992, Vapour-absent melting at 10 kbar of a biotite- and amphibole-bearing tonalitic gneiss: Implications for the generation of A-type granites. Geology, v. 20, p. 263-266.
- Srogi, L., Wagner, M.E. and Lutz, T.M., 1993, Dehydration partial melting and disequilibrium in the granulite-facies Wilmington Complex, Pennsylvania-Delaware Piedmont. American Journal of Science, v. 293, p. 405-462.
- Stevens, G. and Van Reenen, D.D., 1992, Partial melting and the origin of the metapelitic granulites in the Southern Marginal Zone of the Limpopo Belt, South Africa. Precambrian Research, v. 55, p. 303-319.
- Stevens, G., Clemens, J.D. and Droop, G.T.R.. 1995, Hydrous cordierite in granulites and crustal magma production. Geology, v. 23, p. 925-928.
- Thompson, A.B., 1976, Mineral reactions in pelitic rocks: II Calculation of some P-T-X(Fe-Mg) phase relations. American Journal of Science, v. 278, p. 425-454.
- Thompson, A.B., 1982, Dehydration melting of pelitic rocks and the generation of H₂O-undersaturated granitic liquids. American Journal of Science, v. 282, p. 1567-1595.
- Turnock, A.C. and Eugster H.P., 1962, Fe-Al oxides: phase relationships below 1000 °C. Magnetite solid solution at high temperature. Journal of Petrology, v.3, p. 533-539.
- Vielzeuf, D. and Holloway, J.R., 1988, Experimental determination of the fluid-absent melting reactions in the pelitic system. Consequences for crustal differentiation. Contributions to

Mineralogy and Petrology, v. 98, p. 257-276.

Vielzeuf, D., Clemens, J.D. and Pin, C., 1990, Granites, granulites and crustal differentiation. In, Vielzeuf, D. and Vidal, P. (eds), *Granulites and Crustal Evolution*, Kluwer Academic Publishers, Dordrecht, p. 59-86.

Vielzeuf, D. and Clemens, J.D., 1992, The fluid-absent melting of phlogopite + quartz. Experiments and models. *American Mineralogist*, v. 77, p. 1206-1222.

Vielzeuf, D. and Montel, J-M, 1994, Partial melting of metagreywackes. 1. Fluid-absent experiments and phase relationships. *Contributions to Mineralogy and Petrology*, v. 117, p. 375-393.

Vry, J.K., Brown, P.E. and Valley, J.W., 1990, Cordierite volatile content and the role of CO₂ in high-grade metamorphism. *American Mineralogist*, v. 75, p. 71-88.

Winkler H.G.F., 1976, *Petrogenesis of Metamorphic Rocks*, 4th edn, Springer-Verlag, New York, 334 pp.